PARAMETERS AFFECTING THE MEASUREMENT OF
HYDRAULIC CONDUCTIVITY FOR SOLIDIFIED/STABILIZED WASTES

by

D.J. Conrad, S.A. Shumborski, L.Z. Florence, A.J. Liem
Alberta Environmental Centre
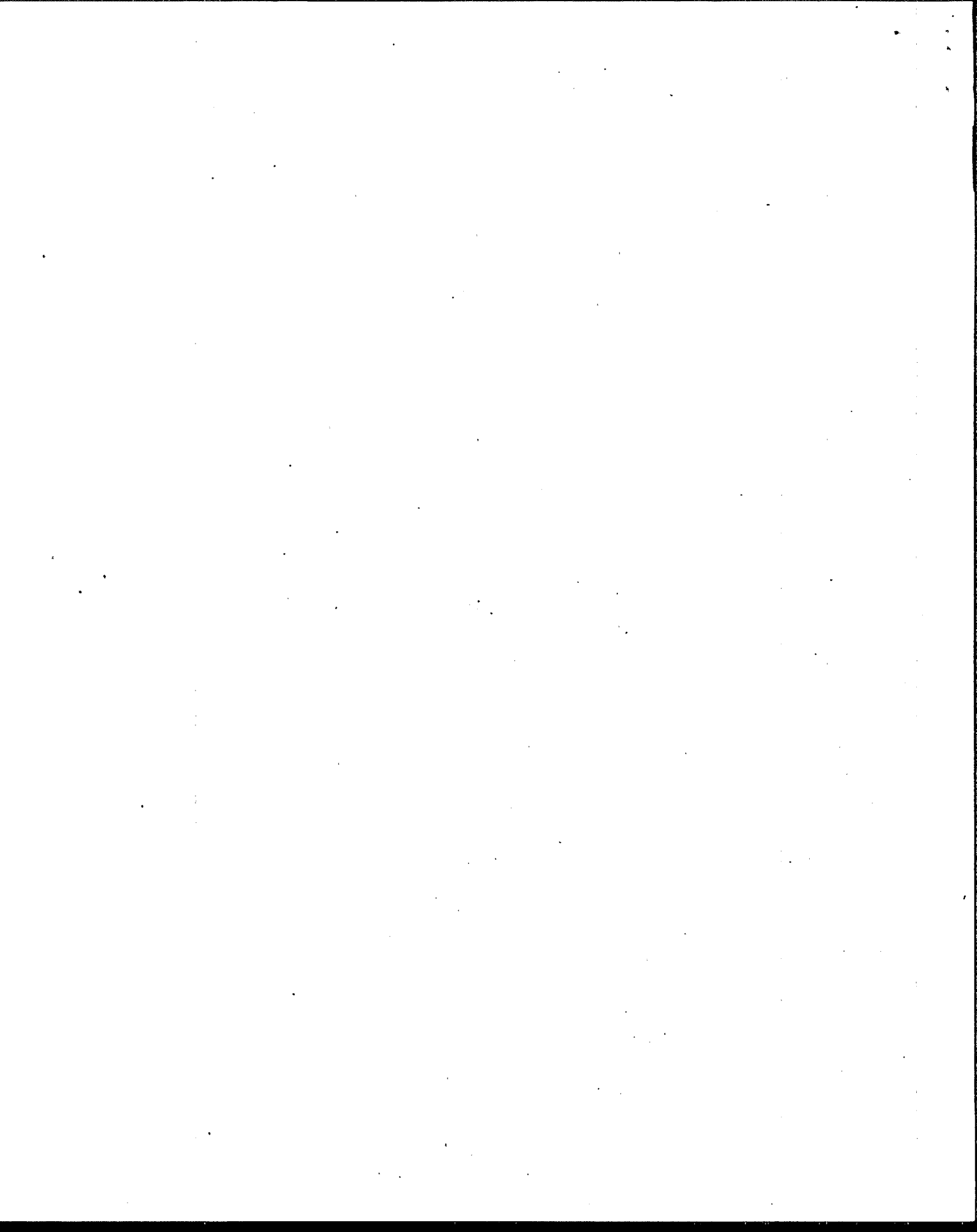Vegreville, Alberta, Canada   TOB 4LO

CR814860-01-1

Project Officer

NOTICE

The information in this document has been funded in part by the U.S. Environmental Protection Agency under Cooperative Agreement # CR814860-01 with the Alberta Environmental Centre, Vegreville, Alberta, Canada. It has been subjected to the Agency's peer and administrative review and approved for publication as an EPA document. Mention of trade names or commercial products does not constitute endorsement or recommendation for use.
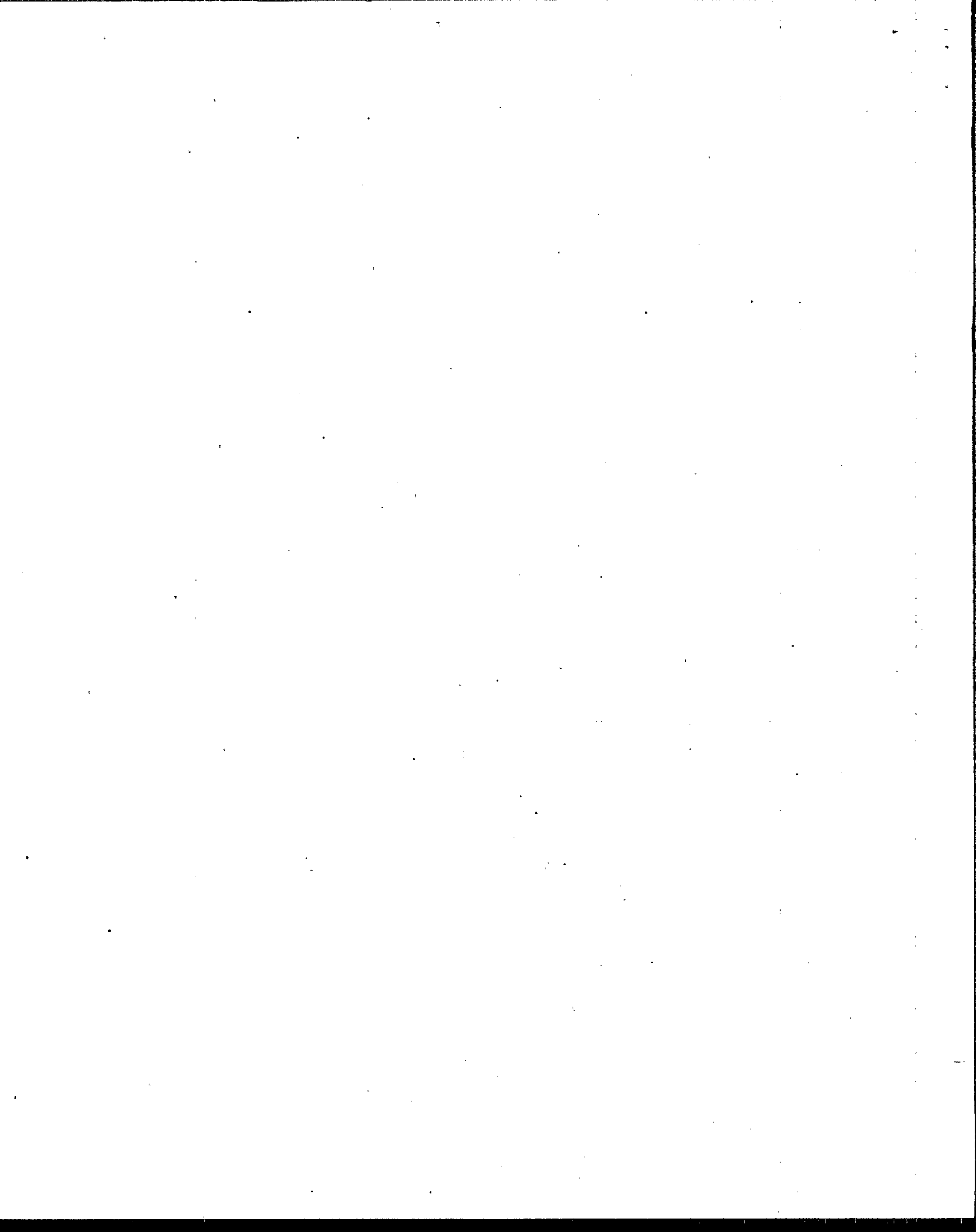
FOREWORD

Today's rapidly developing and changing technologies and industrial products and practices frequently carry with them the increased generation of materials that, if improperly dealt with, can threaten both public health and the environment. The U.S. Environmental Protection Agency is charged by Congress with protecting the Nation's land, air, and water resources. Under a mandate of national environmental laws, the Agency strives to formulate and implement actions leading to a compatible balance between improving the quality of life and minimizing the risks to the environment. These laws direct the EPA to perform research to define our environmental problems, measure the impacts, and search for solutions.

The Risk Reduction Engineering Laboratory is responsible for planning, implementing, and managing research, development, and demonstration programs to provide an authoritative and defensible information that can be used by both regulators and the regulated in their common efforts to protect the environment from the hazards of industrial and municipal waste. This publication is one of the products of that research and provides a vital communication between the researcher and the user community.

This report describes the effects of varying cement content on the hydraulic conductivity of a solidified hazardous waste. The goal of this work is to gain a better understanding of the mobility of constituents of solidified/stabilized hazardous waste and how to minimize that mobility. This information should be of assistance to regulators and businesses subjected to the waste management requirements of the Resource Conservation and Recovery Act.

E. Timothy Oppelt, Director
Risk Reduction Engineering Laboratory

ABSTRACT

A series of experiments conducted at the Alberta Environmental Centre examined the variation in hydraulic conductivity (K) within and among three matrices formed by steel mill baghouse dust treated with 8%, 9% and 10% Normal Portland Cement at a water/cement ratio of 1:1. Within the 8% and 9% matrices, test gradient (i) and back pressure (P) were combined into 3 x 3 factorial treatments. Commercially available equipment was modified to allow sensitive and continuous monitoring of hydraulic conductivity. A permeant-matrix interaction was indicated by K decreasing with time at a rate which increased with higher cement contents. After hydraulic conductivity testing, the samples were examined by scanning electron microscopy and energy dispersive x-ray analysis. A cement hydration product, identified as ettringite, had formed in the solidified/stabilized waste pores. This product reduced hydraulic conductivity by two orders of magnitude by restricting conducting pores. Four to seven weeks of testing were required before an acceptable equilibrium had been reached and statistical comparisons among the i x P treatments were made. Within each matrix, gradient was statistically the most significant parameter accounting for 60% of the variation in results. The response to gradient was different than that observed with clay and soil-liners in the literature. The overall mean hydraulic conductivity ($p \leq 0.01$) of the 8% matrix ($10 \pm 5 \times 10^{-6}$ cm.sec^{-1}) was significantly greater than that of the 9% matrix ($0.06 \pm 0.03 \times 10^{-6}$ cm.sec^{-1}) ($p \leq 0.01$).

Temporal effects, gradient and cement content were identified as important factors affecting hydraulic conductivity measurements and must be considered by regulatory tests. Bulk density was a useful quality control criterion for minimizing sample variance within each matrix.

CONTENTS

FIGURES

TABLES

ACKNOWLEDGEMENTS

SECTION 1.0

INTRODUCTION

Solidification and stabilization (SS) technologies are often used to treat hazardous wastes to reduce the environmental impact of their disposal. Solidification removes free water, usually by the hydration reactions of lime or cementitious materials, producing a monolithic solid with reduced surface area. Stabilization with cementitious materials reduces the solubility of wastes by the alkaline precipitation of metal hydroxides or metal incorporation into the hydration products of cement.

The long term behaviour of these treated wastes is the subject of much concern. Depending on the disposal scenario, treated wastes are eventually subject to leaching by ground water, precipitation, or leachate. If the treated waste is relatively permeable, leachant flow will be through the whole of the material rather than being confined to the external surface area. Thus, a major benefit of SS treatment, the reduction of surface area available for leaching is compromised.

The flow of liquid through a porous medium is described by Darcy's Law. The liquid superficial velocity (Flowrate/Area) per unit gradient is defined as hydraulic conductivity, which is a function of the properties of the medium and the liquid. Gradient is defined as the headloss which occurs over the sample (cm of H_2O) divided by the sample length (cm). Darcy's Law may be written as:

$$K = \frac{Q}{iA}$$

where K is hydraulic conductivity ($cm.sec^{-1}$), Q is flow rate ($cm^3.sec^{-1}$), i is gradient (dimensionless) and A is cross-sectional area (cm^2).

Permeability, a property of the medium alone, is related to hydraulic conductivity by the following relationship:

$$\kappa = \frac{K\mu}{\rho g}$$

where κ is permeability (cm^2), μ is absolute viscosity of the liquid (g.cm^{-1}.sec^{-1}), ρ is density of the liquid (g.cm^{-3}) and g is acceleration of gravity (980 cm.sec^{-2}).

When there is no medium-liquid interaction, permeability is an intrinsic and useful property of a medium. The flow rates of different liquids through a medium can be readily predicted from its permeability and the properties of the liquids. However, when there are changes in liquid properties, due to dissolution, or in the internal structure of the medium, as shown in this paper, the meaning of permeability becomes obscure. Since it is the flow rate of aqueous permeant through SS waste which is of environmental interest, hydraulic conductivity is the proper terminology and is used herein.

The literature available on hydraulic conductivity measurement with environmental implications deals predominantly with clay and soil liners. Researchers are interested in the effects of permeants, specifically inorganic salt solutions (1), organic fluids (2) and landfill leachates (3). Test parameters such as saturation (4), temporal effects (5, 6) and gradient (6, 7) have been studied.

The corresponding information on solidified/stabilized waste is, however, practically non-existent. Nor is there sufficient information which addresses the differences between clay or soil liners and solidified/stabilized waste, such as compressive strength and permeant-matrix interactions.

This report deals with the effects of parameters affecting the measurement of hydraulic conductivity of solidified/stabilized waste. The study was undertaken to form bases for the development of a regulatory test method - to improve intra and inter-laboratory precision - and to correlate accelerated laboratory test results to those occurring under field conditions.

The scope of the investigation was confined to the following:

- one waste, steel mill baghouse dust, treated with three portions of Normal Portland Cement to produce a range of hydraulic conductivities similar to those found in commercial solidification/stabilization processes.

- the following test and instrument parameters: sample preparation, temporal effects, gradient and back pressure.

New equipment was acquired and modified to allow for sensitive, accurate and continuous flow measurements. Particular attention was given to minimize variance due to sample preparation, and statistical methods and experimental designs were used to delineate parametric effects. Electron microscopy, chemical analyses and measurements of physical properties were conducted to assist in the interpretation of the observed phenomena.

SECTION 2.0

CONCLUSIONS AND RECOMMENDATIONS

1. Hydraulic conductivity was sensitive to matrix composition. Significantly different hydraulic conductivities were measured between samples differing only by 1% in cement content. The ability to distinguish such samples was attributed to the institution of a strict quality control criterion for sample preparation based on bulk density. The corollary is that the variance of hydraulic conductivity due to sample preparation can be minimized by using that criterion.

2. Hydraulic conductivity decreased with elapsed time during testing. A power function in the form of $y = ax^b$ describes the relationship. The decrease could be explained by long-term cement hydration reactions forming ettringite in the permeant-conducting pores. Although matrix dissolution occurred, no effect was observed over the testing period of up to 80 days.

3. The effects of gradient and back pressure on hydraulic conductivity were the following:

   - Gradient was the most significant parameter and its correlation with hydraulic conductivity was positive, the opposite to that for soil and clay liners. This was attributed to the higher unconfined compressive strength and the corresponding lesser degree of sample consolidation.

   - Medium and high levels of gradient and back pressure were the less sensitive region for hydraulic conductivity measurements. Falling-head permeameters, in which low levels of these parameters are used, are thus operated in the more sensitive region.

   - Over the entire region of the chosen experimental levels, the measured hydraulic conductivities varied by a factor of four or less. Values obtained in the laboratory are thus reasonable estimates of those in the field conditions, provided that compaction and curing conditions are similar.

4. The precision attainable for hydraulic conductivity measurements utilizing the quality control criteria, waste type and instrumentation of this study was improved by nearly 50% over that reported in the literature.

5. An exponential relationship between hydraulic conductivity and sample porosity was shown to be statistically significant. How such a relationship varies with different matrices was not investigated.

Recommendations for regulatory test development:

1. Bulk density should be used as a quality control criterion to reduce variance due to sample preparation.

2. To improve precision, temporal effects should be taken into account and measurements carried out at high levels of gradient and back pressure.

3. To estimate maximum hydraulic conductivity, measurements should be made as soon as the sample is cured.

Recommendations for future work:

1. Different matrices should be tested for morphological changes during testing and improving the confidence in the effect of instrument parameters.

2. Saturation effects should be studied to predict field hydraulic conductivity.

SECTION 3.0

LITERATURE SEARCH

The literature available on hydraulic conductivity measurement with environmental implications deals predominantly with clay and soil-liners. Few references exist in the literature concerning the measurement of hydraulic conductivity of solidified/stabilized wastes. This section will briefly review the available literature in terms of the research undertaken from a variety of sources and the direction it suggests for solidified/stabilized waste.

Clay and soil-liner researchers are interested in the effects of dissolved inorganic and organic materials on clay-liner permeability as measured by changes in permeant velocities.

A study by Ather et al (1) investigated the effects of inorganic permeants upon the hydraulic conductivity of bentonite. Increased ionic strength and cationic valence increased the measured hydraulic conductivity. The Gouy-Chapman double layer model of hydrated ions was used to explain postulated changes in the flocculated nature of the bentonite. The degree of flocculation would affect the permeability of the bentonite clay.

Lentz et al (8) observed changes in hydraulic conductivity due to cation exchange and salt precipitation in a magnesium - montmorillonite clay when an alkaline permeant (NaOH) of pH 13 was used.

Acar et al (2) found that pore size distributions of a kaolinite clay were unaffected by a change in permeant from 0.1 N $CaSO_4$ to an organic fluid. However, organic solvents of low water solubility, such as benzene and nitrobenzene, were found to decrease the measured hydraulic conductivity by three orders of magnitude. Soluble organics, such as phenol and acetone, had minimal effects. Thus, differences in measured hydraulic conductivity were due to the ability of solvents to displace pore water.

The work of the above authors suggests that interactions between permeants and clays have measurable effects on hydraulic conductivity. Bowders (9), discussing the work of Pierce and Witter (10) in determining termination criteria for clay permeability testing, stressed that chemical equilibrium must be established when chemically reactive permeants are used. For clays this would mean monitoring influent and effluent chemical characteristics. Bowders agrees with Pierce and Witter on their termination criteria when water is used as the permeant; one pore volume of flow has been passed and hydraulic conductivity vs cumulative pore volumes cannot be shown to differ significantly from zero.

The degree of sample saturation has been found to affect hydraulic conductivity. Elzeftawy and Cartwright (4) used soil water retention curves to predict hydraulic conductivity. They found that the hydraulic conductivity of a soil at 100% saturation was approximately four orders of magnitude greater than at 50% saturation. Carpenter and Stephenson (6) observed that saturation generally increased during hydraulic conductivity testing.

Temporal effects have been noted. Parker et al (5) observed that the permeability of flyash stabilized soils decreased over 13 days of testing possibly due to a flyash - soil interaction. Carpenter and Stephenson (6) noted decreased hydraulic conductivity for clays over shorter time periods (2 hours).

The effect of applied gradient has been studied. Carpenter and Stephenson (6) and Edil and Erikson (7) both noted that hydraulic conductivity declined for clays as the gradient was increased when flexible wall permeameter cells were used. The authors explained these results as due to sample consolidation. Edil and Erikson (7) noted that at high gradients (290-360) gas bubbles were evolved in the effluent lines. This suggests an alternative explanation. High pressure drops across a sample produce unsaturated conditions, due to liquid degassing, which result in decreased hydraulic conductivity.

Bryant and Bodocsi (11) collected historical data on hydraulic conductivity measurements for clay liners and analyzed them for the effects of sample variation, preparation, equilibration and gradient. They noted many confounding effects, and suggested that suitable experimental designs should be chosen to properly estimate parametric effects. Longer test periods and statistical approaches to determine equilibrium, as indicated by stable hydraulic conductivity, were suggested. Soil hydraulic conductivity was found to be very sensitive to preparation technique. Some results showing decreased hydraulic conductivity were explained by sample consolidation resulting from increased gradients.

Pierce et al (12), who conducted ruggedness tests using both rigid wall and triaxial cell permeameters, found that water content, lift thickness and back pressure had the greatest effect on the measured hydraulic conductivity of a clay liner. The first two factors pertain to sample preparation while the third is an instrument measurement parameter. Gradient was not found to be significant at relatively high levels ($i = 100, 200$), typical of laboratory tests. The hydraulic conductivity results exhibited large variability. Thus, inter-laboratory results could exhibit large variation due to individual laboratories performing hydraulic conductivity tests at different levels of these sensitive parameters.

Cement and concrete researchers have investigated the permeability of hardened cement pastes, as cement permeability will affect the weathering properties and corrosion of metal reinforcing rods. This work has some applications to solidified/stabilized wastes because low permeability products are desired for both products and industrial cements are often used as solidification/stabilization additives.

Powers et al (13) noted that long term curing of cement pastes revealed a seven order of magnitude decline in permeability compared to that of the fresh paste. This was explained by the fact that cement gel occupies 2.1 times the volume of the unhydrated paste. Thus, long term curing causes discontinuities in capillary porosity (14) and decreased hydraulic conductivity. Patel et al (15) noted a similar phenomena, that large pore fractions decreased while gel (paste) porosity increased during cement hydration. Later research has attempted

to develop models for hydraulic conductivity based on pore parameters. Nyame and Illston (16) described their hydraulic conductivity data in terms of hydraulic radius theory. Hughes (17) considered pore isotropy and tortuosity in developing a hydraulic conductivity model.

Stegemann and Cote (18) included hydraulic conductivity in an inter-laboratory evaluation of solidified/stabilized waste. A falling head method with a triaxial cell was used to measure hydraulic conductivity for thirty-seven waste samples. Commercially available solidification/stabilization treatment processes yielded hydraulic conductivities between 3×10^{-4} and 7×10^{-8} cm.sec^{-1}. At the interlaboratory level, the variance was too large to determine differences between individual products. A pooled estimate of intralaboratory variance (which does not include the systematic error of each laboratory) was made. Four replicates of the test were estimated to yield a one order of magnitude precision at the 95% confidence level. (Based on a log-normal data distribution, the actual precision is x/$\div$ 7.3.)

Stegemann and Cote (18) felt that "differences between specimens of the same solidified product appeared to be the main cause of the variability observed for this method". This indicates waste heterogeneity and sample preparation as sources of variance. Bulk density is one measure of sample homogeneity. Stegemann and Cote (18) reported a precision for bulk density of ± 0.14 g.cm^{-3} for three replicates of the 95% confidence level. This would correspond to a relative standard deviation of 3.9% at the reported median of 1.44 g.cm^{-3}.

In summary, a review of the pertinent literature suggests several areas of consideration. Clay and soil-liner research indicates that the instrument parameters of gradient and back pressure, as well as sample preparation and temporal considerations, should be elements of a hydraulic conductivity study. Cement research indicates that cement hydration reactions continue over a long time period. A study of solidified/stabilized waste indicates that, on an interlaboratory and intralaboratory level, hydraulic conductivity as practiced offers poor precision, but that this may largely be due to sample variance.

SECTION 4.0

MATERIALS AND METHODS

RAW MATERIALS

The following raw materials were used to produce the surrogate solidified/stabilized waste studied:

1. Steel Mill Baghouse Dust

2. 16 - 30 mesh silica sand (Badger/Cardium Service and Supply)

3. ASTM Type I Normal Portland Cement (Canada Cement Lafarge)

4. Tap Water (North Saskatchewan River, conventional solids removal and partial lime softening; typical finished water pH 8.5, hardness 100 ppm as $CaCO_3$)

SAMPLE PREPARATION AND ACCEPTANCE

The sample formulations, shown in Table 1 were chosen to give a range of hydraulic conductivities typical of solidified/stabilized wastes (10^{-6} to 10^{-8} cm.sec^{-1}).

Samples were prepared by adding weighed portions of the dry ingredients to a Hobart (Model N-50) mixer and mixing for two minutes at low speed (62 rpm, 139 rpm planetary). The required water was added and mixing continued for two minutes with three pauses to scrape material from the side of the mixing bowl.

Table 1. Hydraulic Conductivity Sample Preparations

Matrix	Steelmill Foundry Dust (wt.%)	Silica Sand (wt.%)	Type 1 Portland Cement (wt.%)	Water (wt.%)
8%	42.0	42.0	8.0	8.0
9%	41.0	41.0	9.0	9.0
10%	40.0	40.0	10.0	10.0

Samples were compacted in plastic molds (M.A. Industries, Peachtree, Georgia) using method ASTM D558-82 (19), modified for the smaller sample size according to Table 2. The modified sample preparation support and tamping bar are detailed in Figures 1 and 2 respectively.

Table 2. Sample Compaction Procedure Modifications

		Present Study	ASTM D558-82
Mold:	Diameter (cm)	7.62	10.16
	Height (cm)	15.2	11.643
	Volume (cm^3)	693	944
Sample:	Compacted Height (cm)	16.5	12.7
	No. of lifts	3	3
	Blows/layer	25	25
Rammer:	Diameter (cm)	3.805	5.08
	Area (cm^2)	11.37	20.30
	Mass (g)	1390	2490
	Drop (cm)	30.48	30.48
Compactive Energy (J.cm^{-3})		0.448	0.591

SAMPLE PREPARATION SUPPORT
Drawing # CW3-3*01

8 3/8" X 3" X S PIPE

2" X 2"

SCALE: 1:2

3/8" dia. THREADED @ 10.7cm RADIUS

3/8" dia. UNC

135mm

SCALE: 1:4

2 3/8" ±1/8

2.99" ±0.02"

3.170" +0.015" / -0.005"

1/8" R typ.

2.90" +0.02"

1/32"

6.00" +0.02"

3/8" dia. X 1/2" UNC BOLT

3/4" X 10" MILD STEEL PLATE

1/2 — 1

3/8"

3/8" BOLT WITH WING ATTACHED

FIGURE 1. Modified Sample Preparation Support

The following labels and dimensions appear within the figure:

- 15.4mm
- 28.5mm dia.
- 6.5mm
- 13mm
- 6mm
- 8.5mm – 3/8" X 24 NF
- 9.5mm dia. X 390mm MILD STEEL BAR
- 8.5mm – 3/8" X 24 NF
- 2.8mm X 37.75mm
- 3/8" X 24 NF DRILLED & THREADED
- – Threaded rod inserted to get total weight of tamper = 1392g
- 122.5mm
- 38.05mm dia.
- 10mm
- 6.2mm disk soldered inside the copper pipe
- 20mm
- 6.2mm
- 436mm
- 4 @ 90° X 9.5mm dia typ.
- 20mm
- 41.3mm O.D. X 38.3mm I.D. COPPER PIPE (1-1/2")

FIGURE 2. Modified Tamping Bar

- 13 -

Samples were leveled to the top of the mold with a metal straight edge and cured at 95% min. relative humidity at 23°C for a minimum of 28 days.

After curing, samples were removed from their molds, trimmed to ensure parallel end faces and their physical dimensions and mass determined prior to hydraulic conductivity testing.

INSTRUMENTATION

Three flexible wall permeameters (Geotest Model S5425) were used in this study. Materials of construction were compatible with hazardous waste testing. Metal parts in contact with permeants were stainless steel (type 316). Permeant flow lines were made of teflon and permeant interfaces were teflon-lined. The piston interface was sealed with Viton "o-rings". The permeameters were modified by the substitution of the Transtek #0243 linear variable displacement transducers, with Mitutoyo Digimatic Indicators Type ID-130ME (accuracy of 0.001 mm over a 30 mm range) to measure interface piston displacement. Digitized signals of interface displacements were recorded by a Mitutoyo DP2-DX miniprocessor, which is capable of storing up to 678 displacement and time records. An additional modification was the introduction of a Brainard Kilman model S-545 bladder interface. This modification isolated the air pressurization system from permeameter cell water. A schematic of the permeameter/interface/datalogger arrangement is shown in Figure 3. Details of interface calibration are given in Appendix A.

Permeameter system pressures were measured by a Shape Instruments Ltd pressure transducer model #SP1020 and displayed on a Shape Instruments Ltd transmitter model #SD7500/C. The pressure measuring system was calibrated with a dead weight tester.

Results were downloaded to a Fujikama Model #fK 286 MT computer using in-house produced software.. The computer program is described in Appendix B.

GEOTEST INSTRUMENT CORP.
MODEL S5425 PERMEAMETER

SUPPLY PRESSURE GAUGE

SUPPLY PRESSURE

HEAD PRESSURE REGULATOR

MAIN AIR PRESSURE SUPPLY VALVE

SUPPLY PRESSURE

BACK PRESSURE GAUGE

CELL PRESSURE REGULATOR

BACK PRESSURE REGULATOR

CELL PRESSURE GAUGE

CELL / BACK PRESSURE MEASUREMENT SELECTOR VALVE

BACK PRESSURE SUPPLY VALVE

PEDESTAL INTERFACE VENT VALVE

PEDESTAL INTERFACE SUPPLY VALVE SUPPLY VALVE

HEAD / BACK PRESSURE MEASUREMENT SELECTOR VALVE

CAP INTERFACE HEAD / BACK PRESSURE SELECTOR VALVE

PEDESTAL HEAD / BACK PRESSURE SELECTOR VALVE

TO DATALOGGER

DISPLACEMENT INDICATOR

PEDESTAL INTERFACE

INTERFACE FILLING & DRAINING VALVE

FLOW VALVE

PEDESTAL PURGE VALVE

CAP PURGE VALVE

CELL WATER VALVE

CAP INTERFACE SUPPLY VALVE

TO DATALOGGER

DISPLACEMENT INDICATOR

CAP INTERFACE

INTERFACE FILLING & DRAINING VALVE

FLOW VALVE

CAP INTERFACE VENT VALVE

- 15 -

FIGURE 3. Schematic of Hydraulic Conductivity Apparatus

SAMPLE SATURATION

Cured and trimmed samples were inserted into a latex membrane capped with porous stainless steel disks ($K > 1 \times 10^{-4}$ cm.sec^{-1}) and mounted on the permeameter pedestal. A layer of aluminum foil covered with vacuum grease (for caustic corrosion protection) and a second latex membrane were added to provide a barrier to gas diffusion into the sample from the cell water. Details of the modified flexible wall membrane are shown in Figure 4.

Samples were saturated by evacuating the sample for one hour from the outlet side with a model D150 Precision vacuum pump protected by a liquid nitrogen cold trap. Degassed water was introduced to the evacuated sample from the inlet end to begin saturation and completed with the permeant pressurized to 7 kPa.

SAMPLE POROSITY

Sample porosity is defined as the ratio of interstitial volume to the total sample volume. For a granular solid in the liquid saturated state, porosity is one of the parameters affecting headloss and thus flow rate. Porosity, (E, - dimensionless) may be determined by the following relationship:

$$E = 1 - \frac{\rho_B}{\rho} (1 - W)$$

where ρ_B is the wet sample bulk density (g.cm^{-3}), ρ is the density of the solids or "true density" (g.cm^{-3}) and W is the proportion of water content in the sample (dimensionless).

The actual pore volume (PV) in cm^3 may be determined by:

$$PV = Vs - \frac{Ms (1 - W)}{\rho}$$

where Vs is the sample volume (cm^3) and Ms is the mass of the wet sample (g).

SAMPLE CHARACTERIZATION

The methods used to measure the physical characteristics of the hydraulic conductivity samples and the exuded permeants are listed in Table 3.

ELECTRON MICROSCOPY

Electron microscopical analyses were performed on a Hitachi S510 scanning electron microscope (SEM), a Hitachi X-650 (SEM) with energy dispersive x-ray spectrometer and a Hitachi H-600 scanning transmission electron microscope (STEM) equipped with a Kevex Be window X-ray detector.

CHEMICAL ANALYSES

Chemical analyses of the foundry baghouse dust and exuded permeants was performed utilizing the methods of ion coupled spectroscopy, atomic absorption spectroscopy, colorimetry and potentiometric titration.

SCALE: 3:1 (3X)

LATEX MEMBRANE

VACUUM GREASE

ALUMINUM FOIL (0.023mm)

'O' RING

CAP

Porous
Stainless
Steel

SAMPLE

Porous
Stainless
Steel

PEDESTAL
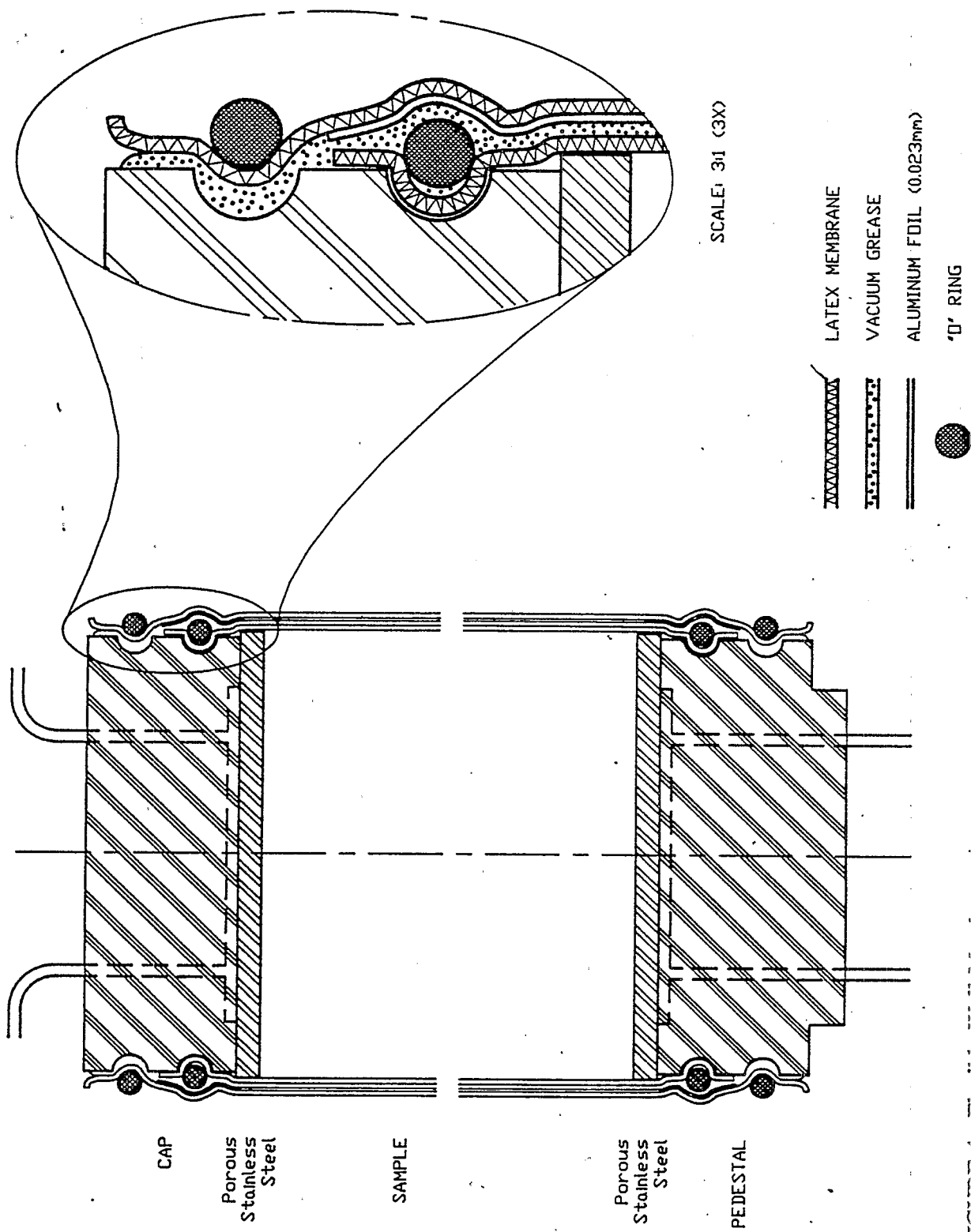
FIGURE 4. Flexible Wall Membrane Arrangement

- 18 -

Table 3. Physical Test Methods

Parameter	Method	Modifications
Moisture	ASTM D2216-80 (20) Standard Method for Laboratory Determination of Water Content of Soil, Rock and Soil Aggregate Mixtures	60°C constant weight
Bulk Density	ASTM D558-82 (19) Standard Test Methods for Moisture-Density Relations of Soil-Cement Mixtures	See Table 2
True Density	ASTM C604-86 (21) Standard Test Method for True Specific Gravity of Refractory Materials by Gas-Comparison Pycnometer	Dried at 60°C, ground to pass a 1.18 mm screen.
Unconfined Compressive Strength	ASTM D1633-84 (22) Standard Test Method for Compressive Strength of Molded Soil-Cement Cylinders.	Tested at 2.5 mm/min.
Total Solids	AWWA #209A (23) Total Residue Dried at 103 - 105°C	

SECTION 5.0

EXPERIMENTAL PROCEDURES

SAMPLE PREPARATION AND ACCEPTANCE

Samples for hydraulic conductivity testing were prepared for each matrix in batches of approximately eight samples. Samples accepted for testing met a quality assurance criteria of ± 0.5% of the mean of batch bulk density. (See Bulk Density Measurements in Results and Discussion)

HYDRAULIC CONDUCTIVITY DATA RECORDING

Initial measurements were conducted at median experimental levels of gradient (116) and back pressure (69 kPa). Data were recorded when inflow and outflow rates were determined to be within 5%.

DETERMINATION OF HYDRAULIC CONDUCTIVITY EQUILIBRIUM CONDITIONS

Simple, linear regression was used to identify the time (x = day = independent variable) when changes in hydraulic conductivity ($y = K \cdot 10^6$ = dependent variable) had attained sufficient stable equilibrium that the regression coefficient, or slope, was not different than zero, as suggested by Pierce and Witter (10).

Three 8% matrix samples were tested concurrently on the three Geotest permeameters of median levels of gradient and back pressure over a twenty-nine day period. Their measured hydraulic conductivity was compared to that predicted from the equation derived previously for the 8% matrix.

EXPERIMENTAL DESIGN

Gradient and back pressure were varied and treated as independent continuous variables at three levels in a completely randomized 3 x 3 factorial design (see Table 4). Gradient levels corresponded to pressures of 10 kPa to 340 kPa. Two independent experiments were performed at 8%, and 9% matrix to provide a range of hydraulic conductivities. Second-degree polynomial coefficients were calculated using response surface regression (SAS 1988 Release 6.03 (24)) to model the response of hydraulic conductivity to varying levels of gradient and back pressure.

Table 4. Test Parameters and Levels[+]

Parameter	Level		
	-1	0	+1
Gradient	8	116	227
Back Pressure (kPa)	14	69	124

[+] Performed at 8% and 9% matrix

PHYSICAL CHARACTERISTICS

Companion samples were tested for the criteria listed in Table 3, before commencing hydraulic conductivity testing, to determine the initial porosity, saturation and unconfined compressive strength. Hydraulic conductivity samples were tested for the same criteria to determine if changes in physical characteristics could account for the changes observed in hydraulic conductivity.

RESULTS AND DISCUSSION

CHOICE OF RAW MATERIALS

The raw materials used were chosen for this study to fulfill the following criteria:

1)   the waste material should be produced in high volume, be amenable to solidification/stabilization treatment and have wide concern in terms of North American industry;

2)   the solidification/stabilization treatment should be in common use and generic rather than proprietary;

3)   the solidified/stabilized waste treatments should produce values of measured hydraulic conductivity typical of commercially treated solidified/stabilized wastes.

The waste material chosen was a baghouse dust collected from a steel mill particulate emission control system. Baghouse dusts constitute a large portion of the 9000 tonnes of wastes produced annually by the foundry industry in Alberta (population 2.4 million). A nitric acid digestate of the baghouse dust used in this study was analyzed with an ion coupled plasma spectrometer. Analyses are summarized in Table 5.

Table 5. Baghouse Dust Metal Analyses

Metal	No. of Samples	Mean (mg/kg)	Standard Deviation (mg/kg)
Fe	3	372000	5240
Zn	3	53700	762
Pb	3	9740	552
Cu	3	2510	44
Cr	3	1450	19

This waste, consisting of environmentally sensitive heavy metals in an inorganic matrix, is suitable for treatment by solidification/stabilization technologies. Foundry dusts are classified in Canada under the Transportation of Dangerous Goods Act as Waste Type 80. In the United States the EPA specifies emission control dusts and sludges from the electric furnace production of steel under Hazardous Waste No. K 061.

The solidification/stabilization treatment chosen for this study utilized ASTM Type I Normal Portland Cement. Cement treatment of wastes is widely practiced.

During preliminary sample preparation studies it was noted that swelling and surface cracking of the samples occurred during curing. Samples which remained intact during curing demonstrated very low hydraulic conductivities ($\approx 10^{-10}$ cm.sec^{-1}).

Diluting the baghouse dust with 16 - 30 mesh silica sand allowed a range of cement treatment levels to be tested without sample swelling and cracking. Furthermore, this addition of silica sand allowed samples with a range of hydraulic conductivities to be tested.

BULK DENSITY MEASUREMENTS

The samples prepared in this study had the consistency of soil-cement and thus a standard compaction method for soil cements was used. Bulk density measurements of these samples are summarized in Table 6.

Table 6. Sample Bulk Densities

Matrix	8%	9%	10%
n[+]	16	18	16
Bulk Density ($g.cm^{-3}$) Mean	2.398	2.480	2.527
Standard Deviation	0.024	0.043	0.009
Relative Standard Deviation (%)	1.00	1.73	0.363

[+]n is the number of samples

Results from Table 6 indicate that different nominal matrix content samples may have similar bulk densities even when standard compaction procedures are used. Bulk density is a function of gross sample porosity and has been implicated as a source of variation in hydraulic conductivity measurements. The degree of compaction has been found to affect the measured permeability of clayey silt (25). Stegemann and Cote (18) postulated that sample differences were a major source of variation for hydraulic conductivity in their inter-laboratory comparison study of solidified/stabilized wastes. In this study, a concerted effort was made to minimize this source of variation in order to study only the effects of instrument parameters. Thus, a quality assurance criterion was instituted which rejected all samples with bulk densities not within 0.5% of the sample mean. This criterion ensured that discrete sample populations were obtained for each nominal matrix concentration.

Steady state flow as indicated by equal inflow and outflow rates of permeant was obtained on the first or second day of testing. This steady state flow was measured over several weeks to study if the samples and permeants were in an equilibrium state. Equilibrium would be indicated by no significant change in hydraulic conductivity with time. The results[1] illustrated in Figure 5 show the temporal effects over 80 days of testing at constant gradient and back pressure. All samples displayed a marked and rapid decrease with respect to time. (Note the different scales.) Hydraulic conductivity decreased by nearly two orders of magnitude for the highest cement content sample.

The decrease in hydraulic conductivity was modelled according to the equation:

$$K \times 10^6 = A \, (T + 1)^B$$

where T is the elapsed time measured from the first day of testing (T=0) and A and B are the intercept (initial condition) and slope of the power function, respectively. The regression results are summarized in Table 7, showing the statistical significance of the models.

Table 7. Model Coefficients* for the Change in Hydraulic Conductivity with Time

Matrix	Initial Value (A)	Standard Error	Slope (B)	Standard Error
8%	82.400	±4.361	-0.413	±0.025
9%	1.571	±0.044	-0.743	±0.032
10%	1.356	±0.148	-1.476	±0.070

*regressions are significant at $p<0.001$; the models explain 98% (minimum) of the variation in hydraulic conductivity.

[1]Note: Hydraulic conductivity results are summarized in Appendix C. For the purpose of easy comparison, all hydraulic conductivity measurements discussed in figures and surface response regressions have been multiplied by 1×10^6 unless specified otherwise.
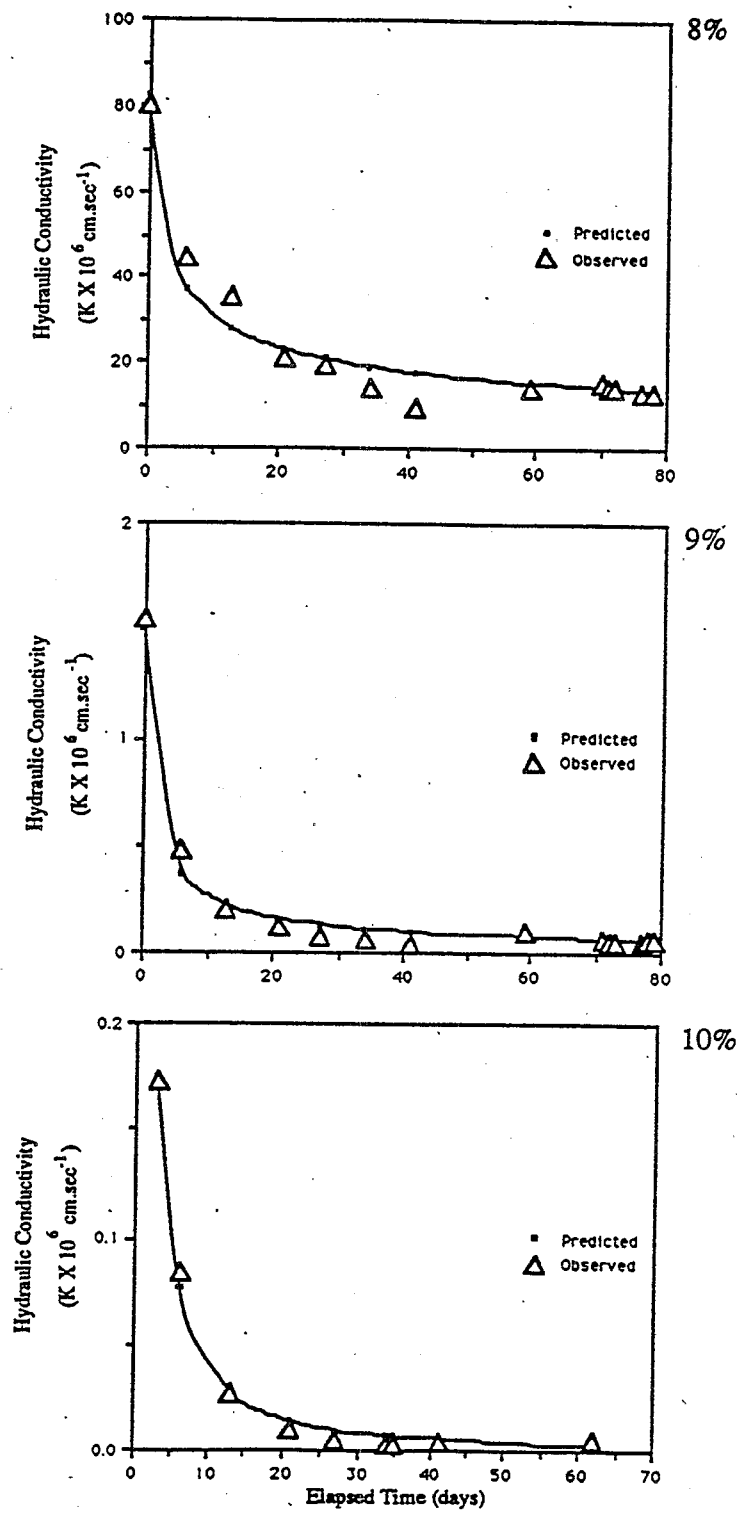
FIGURE 5. Variation of Hydraulic Conductivity With Time at 8%, 9% and 10% Cement

The models are highly significant and explain a large portion of the variation in hydraulic conductivity with time. Temporal effects could be a source of variance within and between laboratories if not accounted for.

The results of hydraulic conductivity suggest that permeants and samples are not in physical/chemical equilibrium, but that some change in physical parameters is occuring.

The models also predict that with time hydraulic conductivity approaches "zero", but, in fact, this will never be achieved. However, if no future dissolution occurred, hydraulic conductivity for the system studied would have a decreased impact on environmental loading. Leaching from sample surfaces and gross defects (cracks) would have the largest impact on waste transport, rather than transport from within the interior by permeant flow.

The hydraulic conductivity results show large differences for the initial conditions between the 8% and 9% matrices (8.24×10^{-5} cm.sec^{-1} vs 1.57×10^{-6} cm.sec^{-1} respectively). The initial conductivity for the 10% matrix (1.36×10^{-6} cm.sec^{-1}) is not significantly different from the 9% matrix. The differences in initial hydraulic conductivity may be due to different mechanisms. The connected porosity of the 8% matrix may be greater than those of the 9% and 10% matrices such that it behaves as a granular material. The 9% and 10% matrices behave as pastes because of their higher cement and water contents.

The change in hydraulic conductivity with respect to time, (the "B" coefficient in Table 7) shows that hydraulic conductivity decreases more rapidly as the cement content increases. This suggests that the aqueous permeant-matrix interactions may be some form of cement hydration reaction which is promoted by passing aqueous permeant through the sample.

The phenomenon of reduced hydraulic conductivity with time has been observed with hardened cement pastes. Powers et al. (13) noted that the hydraulic conductivity of cement pastes cured underwater was reduced by six orders of magnitude due to increased hydration. Powers et al. (14) described the mechanism of this phenomenon. The volume of hydrated

paste is 2.1 times greater than unhydrated paste and hydration products fill pores and cavities, causing discontinuities, effectively reducing the number of flow channels. The number and radii of conducting capillary pores appear to define hydraulic conductivity in cement pastes. Nyame and Illston (16) compared their hydraulic conductivity data to that predicted by hydraulic radius theory and suggested a correlation. Hughes (17) considered the effects of pore characteristics (isotropy and tortuosity) in developing a model for cement-paste hydraulic conductivity, which considered conducting channels as Poiseuille tubes.

Visual inspections of tested samples revealed inclusions of white material in the normally dark solidified/stabilized samples. Examination of the 8% matrix by scanning electron microscopy (SEM) revealed profuse fibrous growth (see Figure 6). Examination of this material at enhanced magnification revealed a material morphologically similar to ettringite ($3CaO.Al_2O_3.CaSO_4.31H_2O$) (see Figure 7) rather than one of the major hydration products of normal portland cement, such as calcium silica hydrate (CSH) or calcium hydroxide (CH).

The morphology of the observed fibres was similar to that of the Aft fibres described by Dalgliesh and Pratt (26). Analysis of individual fibres by SEM with an energy dispersive x-ray spectrometer, revealed the presence of Ca, Al, S and traces of Fe (see Figure 8). This result also suggests the presence of minor cement phases similar to ettringite, specifically the aluminoferrite monosulphate (Afm) and aluminoferrite trisulphate (Aft) phases.

Individual fibres were subsequently analyzed by a scanning transmission electron microscope coupled with an X-ray analyzer. Ca:S ratios were determined to be 2.62 ± 0.52. The trisulphate form and monosulphate form of the aluminoferrites have Ca:S ratios of 2.1 and 4.1 respectively. Thus, the phase found in this solidified/stabilized waste matrix is composed largely of the Aft phase.

FIGURE 6. Fibrous Growth in Tested 8% Matrix (1000X)
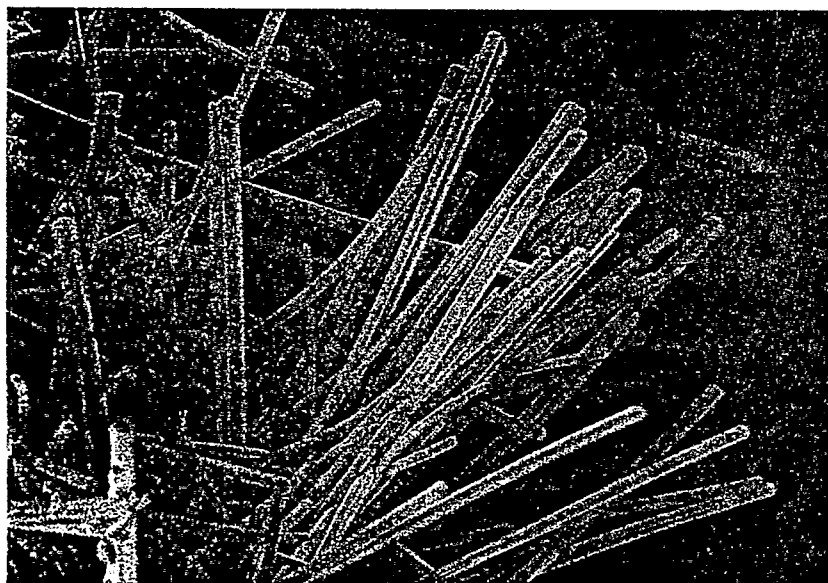
FIGURE 7. Fibrous Growth in Tested 8% Matrix
Showing Morphological Similarities to Ettringite (6000X)
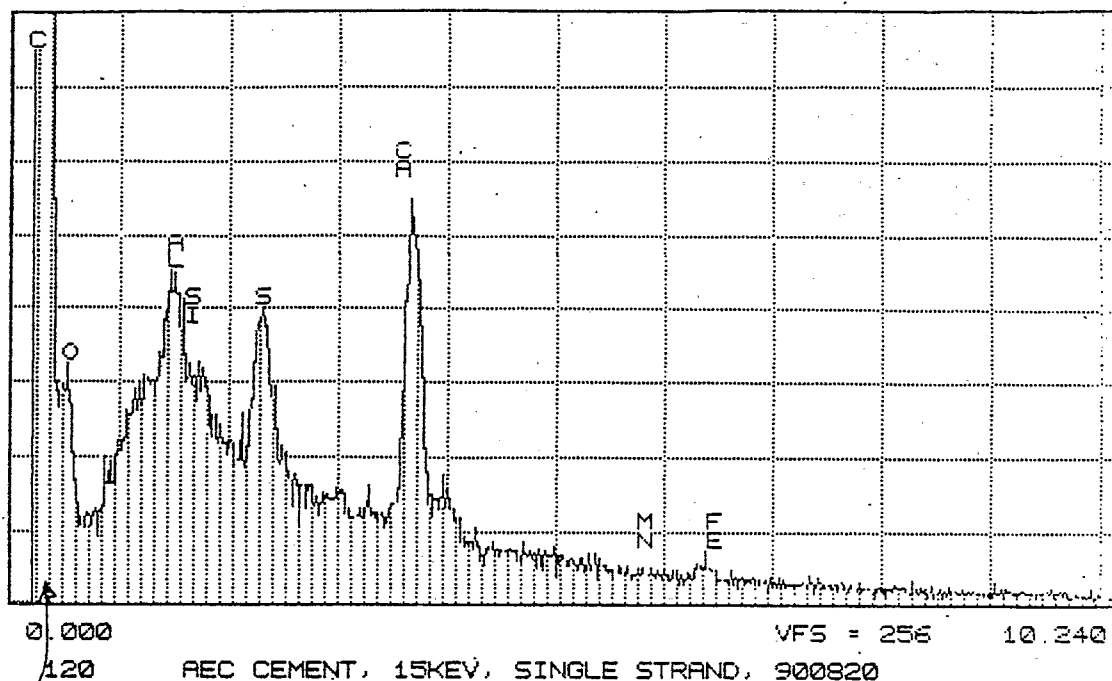
FIGURE 8. X-ray Analysis of Individual Fibres

The ettringite phase was found in all matrices. Figures 9 and 10 show the presence of ettringite in the 9% matrix which formed larger structures and in some cases blocked off pores. Patel et al. (15) noted a similar phenomenon that large pore fractions decreased while gel (paste) porosity increased during cement paste hydration. Figures 11 and 12 show the presence of ettringite in the 10% matrix. No evidence of ettringite was found in companion samples of 8%, 9% and 10% matrices which were cured over a similar time period in a humidity chamber at 95% minimum Relative Humidity, as shown by Figures 13a to 13c.

Control samples containing only 23% Normal Portland Cement, 68% sand and 9% H_2O were cured under water or in an environmental chamber for 28 days. Ettringite was found in the cement samples cured under water (Figure 14) but not in the samples cured in the
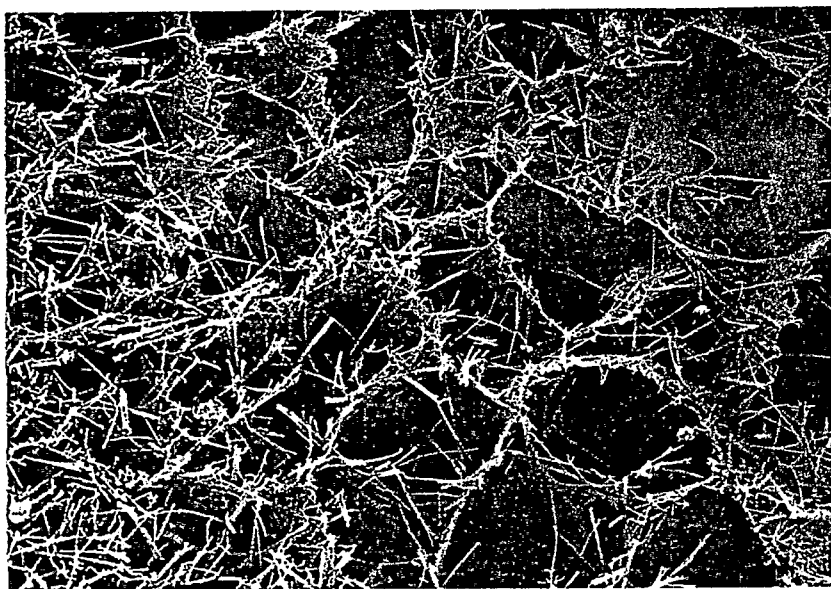
FIGURE 9. Ettringite Growth in Pores of the 9% Matrix Sample (1000X)
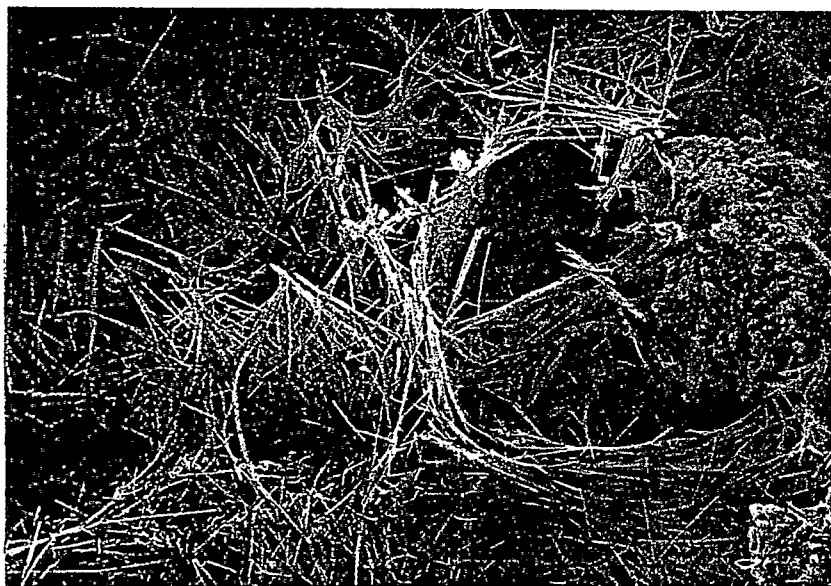
FIGURE 10. Ettringite Growth Blocking Pores in the 9% Matrix Sample (X1000)

environmental chamber (Figure 15). The ettringite appears less profuse in the cement controls and, although this may be partly due to less rigorous hydration; it does suggest that matrix-permeant reactions may promote the formation of ettringite.

The results of hydraulic conductivity and electron microscopy analyses show that cementitious wastes will react intimately with aqueous permeants and that cement hydration reactions continue for some time. This suggests that hydraulic conductivity regulations should consider temporal effects, by specifying sufficient replication over time, to measure permeant-matrix interactions. These interactions will likely vary between SS treatment techniques and should be studied on a case by case basis.

Caution is in order when predicting the long term behaviour of wastes based on short term tests. The hydration reactions discussed above are no doubt promoted by passing water through the samples during testing in an accelerated test. Not all hydration products may prove ultimately beneficial. Ettringite, for example, is formed during the sulphate attack of cements destroying its monolithic properties.

FIGURE 11. Ettringite Growth in the 10% Matrix Pores (X200)

FIGURE 12. Ettringite Growth in the 10% Matrix Pores (X1000)

Figure 13. Samples Cured in Humidity Chamber
Showing No Evidence of Ettringite
a) 8% Matrix b) 9% Matrix
c) 10% Matrix

FIGURE 14. Cement Control Sample Cured Under Water

FIGURE 15. Cement Control Sample Cured in the Humidity Chamber

MODEL TESTING AND TEST PRECISION

The results from testing three 8% matrix samples on three hydraulic conductivity apparatus termed #925, #929 and #930, against the model derived previously for the 8% matrix are shown in Figure 16. The y axis represents the difference between observed and predicted hydraulic conductivity. Thus "zero" on this axis would represent perfect agreement between predicted and observed values. Machine #925 demonstrated a nearly constant difference (-6×10^{-6}). This machine was used to generate the original 8% matrix model and so represents variance between sample preparations. The deviations from the model of machines 928 and 930 reflect variances due to between sample preparation and between machine. Results from Machines 928 and 930 tend to converge to the predicted model values with time. Thus, the temporal changes observed in this solidified waste cause differences in observed hydraulic conductivity between the same matrix samples to become smaller with time.

Figure 17 illustrates the experimental results of hydraulic conductivity for the replicate 8% samples (Raw Data is shown in Appendix C). The graph shows that the range of observed values decreases with time. Table 8 summarizes the means and standard deviations of the log transformed data. A log transformation has been applied by Bryant and Bodocsi (11) for clay and soil-liners and Stegemann and Cote (18) for solidified/stabilized wastes. Bryant and Bodocsi (11) demonstrated that the log of hydraulic conductivity measurements should stabilize variance, are more meaningful because of the large ranges of data, cause sources of variance to become additive rather than multiplicative and simplify relationships between hydraulic conductivity and related quantities such as void ratios. Appendix C shows that after a log transformation of the raw hydraulic conductivity data the null hypothesis of a normal distribution cannot be rejected at ≤ 0.10.

Precision is defined in Table 8 as the 95% confidence limits for the estimate of the mean with three samples. This allows direct comparison of precision estimates for hydraulic conductivity measurements with those obtained by Stegemann and Cote (18) who report a

Table 8. Descriptive Statistics of Log_{10} K for the 8% Matrix Replicates

Test Day	Mean log K	Standard Deviation	Precision*
1	-3.924	0.184	x/÷ 3.80
8	-4.308	0.248	x/÷ 4.40
15	-4.475	0.233	x/÷ 4.25
22	-4.613	0.256	x/÷ 4.48
29	-4.782	0.244	x/÷ 4.36

* 95% confidence limit of mean K for 3 samples

precision of x/÷ 7.3 among four replicates. In this study a precision of x/÷ 4.36 (median estimate) was obtained with only three samples. The estimate in this study contains both machine and sample variance. Recall that a strict quality control criterion was instituted for sample preparation and this is reflected by the small deviation from the model predictions for machine # 925. The hydraulic conductivity measurements were obtained at median levels of gradient and back pressure. It will be shown later that hydraulic conductivity is least sensitive to gradient and back pressure at these levels.

SOLUBILITY EFFECTS DURING TESTING

During hydraulic conductivity testing solidified/stabilized wastes are subject to dissolution by permeants. In the absence of waste/permeant hydration products, as discussed previously, the processes of leaching will enlarge conducting pores, which theoretically should increase sample permeability and measured hydraulic conductivity. The extent of leaching was studied as the surrogate waste chosen did not display this behaviour.

Total dissolved solids (TDS) analysis of effluent from hydraulic conductivity samples were routinely performed for each matrix. Results are illustrated in Figure 18.
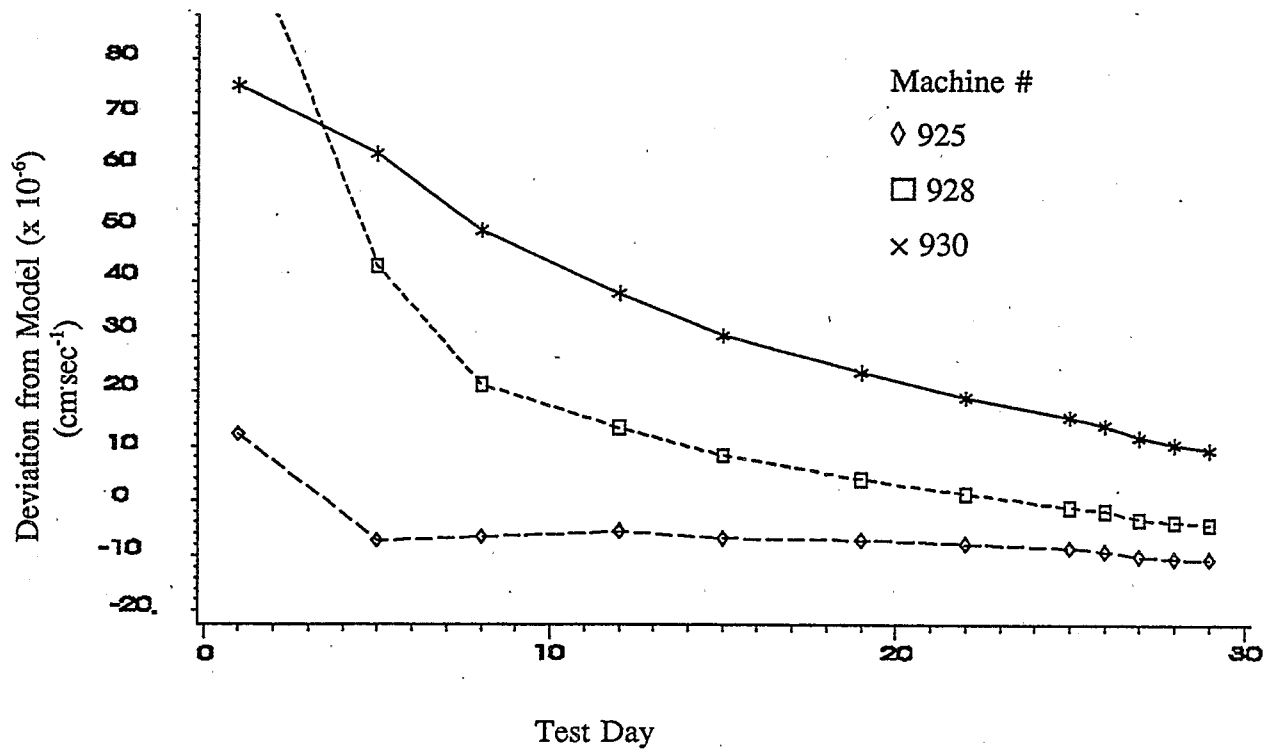
FIGURE 16. Deviation from the Predicted 8% Model
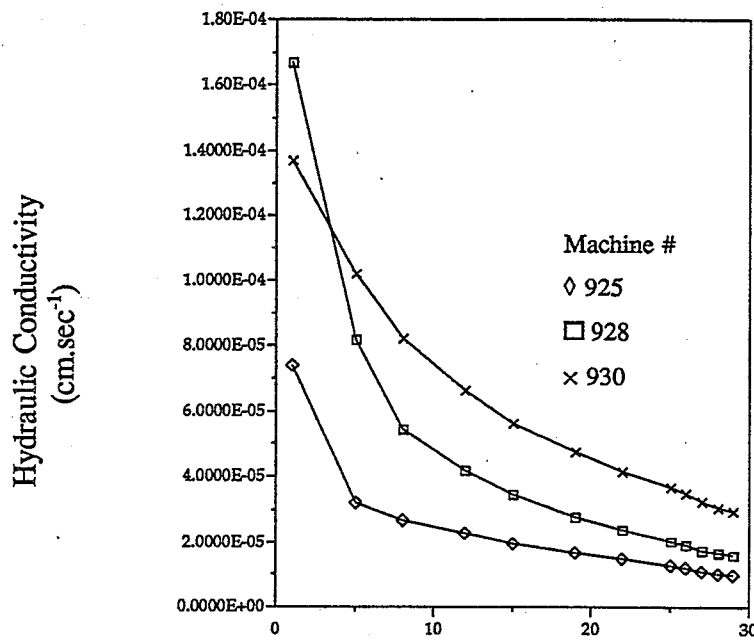
FIGURE 17. Hydraulic Conductivity Replicates for 8% Matrix at Median Levels of i and P
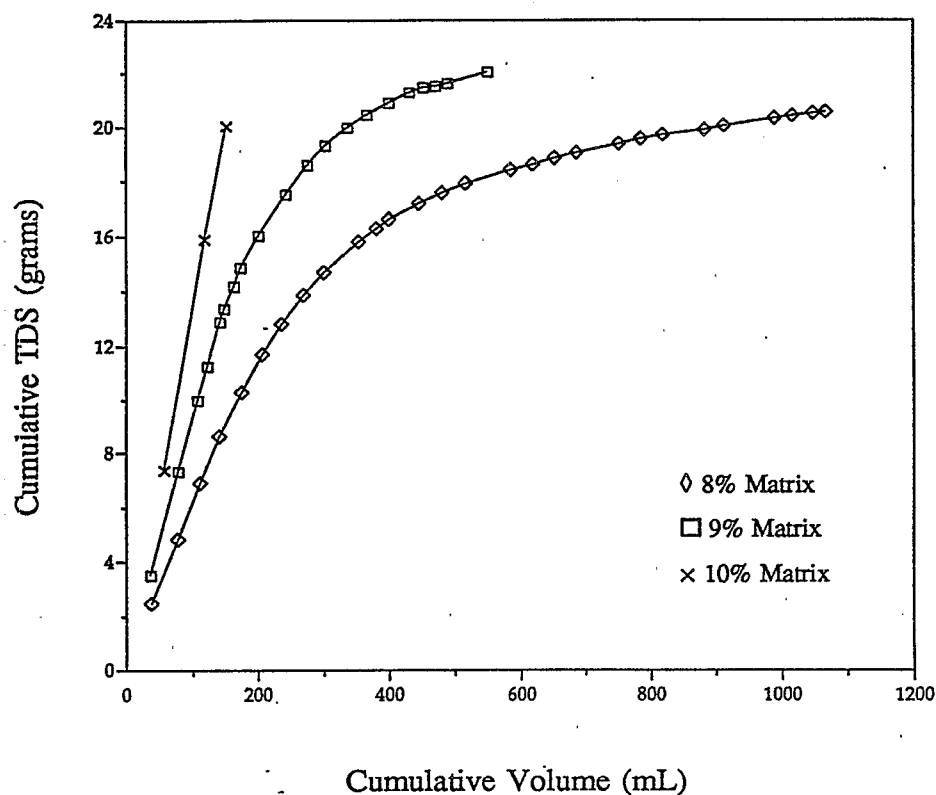
FIGURE 18. Leaching of Hydraulic Conductivity Samples During Testing

A measurable portion of the sample was leached during testing. More than 20 grams of solids were leached from each sample which corresponds to slightly more than 1% of the sample weight. The leaching rate appears to be proportional to the matrix which implicates cement and water content as the controlling parameters for leaching.

Chemical analysis of a composite permeant sample from a 9% matrix scoping sample is shown in Table 9. Analyses show that the permeant is highly basic, and that the freely soluble sulphate, chloride and hydroxide salts of Na and K are the largest components of dissolved solids. Calcium is relatively insoluble at high pH which explains its low value. Zn and Cr analyses are included to demonstrate that amphoteric metals can be quite soluble at high pH.

Table 9. Composite Permeant Analyses of the 9% Matrix

Analyte	Concentration (mg/L)*
pH	14 (standard units)
Na	20800
K	17000
OH-	12300
Cl-	10100
SO_4^{2-}	14900
Ca	59.2
Zn	69.3
Cr	44.0

* Unless specified

Figure 19 shows the relationship between the log of hydraulic conductivity and cumulative total dissolved solids. The graph demonstrates that hydraulic conductivity continues to decline even under conditions which leach alkali which has been attributed to ettringite formation.

A comprehensive explanation for the behaviour of the solidified/stabilized waste is now possible. In low porosity products, produced by low water-contents and no aggregate, ettringite can cause swelling cracks. In the surrogate waste matrix chosen for this study, the added sand increases sample porosity to such an extent that ettringite can form without forming swelling cracks. During hydraulic conductivity testing, soluble alkali, including sulphates, dissolve and attack the tricalcium aluminate phases forming ettringite. This material swells and fills sample pores causing reduced hydraulic conductivity as shown in this study.

The beneficial formation of ettringite may be more specific to this waste matrix than general in application. Waste treatment engineers normally try to minimize sample porosity
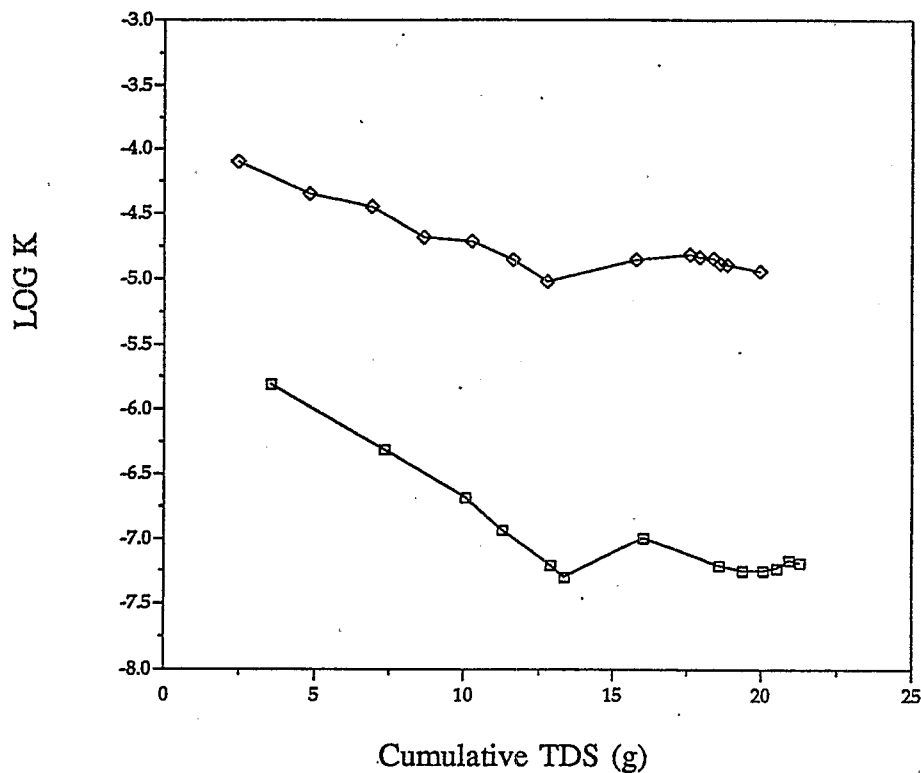
FIGURE 19. Log K vs Cumulative TDS at Median Levels of i and P

and water content. Swelling hydration products, such as ettringite, would cause cracking, resulting in an increase in surface area and hydraulic conductivity.

RESPONSE SURFACE REGRESSION ANALYSES

Effect of Matrix

Hydraulic conductivity data were collected for the 8%, 9% and 10% matrix over 80 days of testing at the various trial levels of gradient and back pressure outlined in the experimental design. The overall mean hydraulic conductivity was significantly greater ($p \leq 0.01$) for the 8% matrix ($10 \pm 5 \times 10^{-6}$ cm.sec^{-1}) compared to the 9% matrix (0.06 ± 0.03

x 10^{-6} cm.sec^{-1}). For the waste system and measurement method chosen, hydraulic conductivity could differentiate between the 8% and 9% matrix treatments even when the confounding factors of time and instrument measurement parameters are retained.

The overall mean of the 10% matrix was not significantly different than the 9% matrix. As discussed previously, the 9% and 10% matrices behave as pastes in sample preparation; but the 8% matrix behaves as a soil-cement (granular solid).

The matrix-permeant interactions caused a decrease in hydraulic conductivity with time. If the differences between matrices are analyzed with non-parametric statistics (sign test) or treated as dependant samples paired according to date and instrument conditions, differences between all matrices would likely become significant.

Hydraulic conductivity has been shown to be very sensitive to matrix for the waste treatment system chosen, if temporal and machine conditions are considered.

Effect of Instrument Parameters

After equilibrium had been reached as indicated by the criteria outlined previously, the variation in hydraulic conductivity with gradient and back pressure was modelled by a second order polynomial:

$$K \times 10^6 = b_0 + b_1 x_1 + b_2 x_2 + b_{11} x^2_1 + b_{22} x^2_2 + b_{12} x_1 x_2$$

where x_1 and x_2 are the coded (-1 to +1) design coefficients of gradient and back pressure, respectively.

Regressions were performed for the 8% and 9% matrices. The 10% matrix reached such a low value of K that single measurements often required more than 1 week of testing. Eight and nine percent matrices could be tested concurrently over much shorter periods. Because our goal was to compare matrices under similar test conditions, the 10% matrix tests were not deemed to be comparable and thus were not included.

The results of the response surface regression analyses are summarized in Table 10 using coded levels of the test parameters.

For the 8% matrix, only gradient has a significant effect on measured hydraulic conductivity. Both linear (b_1 positive) and quadratic (b_{11} negative) terms of gradient are significant. Back pressure at the levels chosen in this experiment did not have a significant effect on measured hydraulic conductivity. Figure 20 shows the values of hydraulic conductivity predicted by the response surface regression as a function of gradient and back pressure using decoded (actual) levels. Hydraulic conductivity is maximized at the median levels of gradient (154) then declines due to the quadratic effect and is minimized at the low levels of gradient. Figure 21 displays a contour plot of hydraulic conductivity from the same model. In addition to predicting maximum values for measured hydraulic conductivity at the median levels of gradient (and back pressure), the hydraulic conductivity intervals (conditions

yielding equal values of K) show that the sensitivity of K to gradient and back pressure is minimized at median levels.

For the 9% matrix, Table 10 shows that only linear terms of gradient (positive) and back pressure (positive) are significant. The effect of gradient is estimated to be double that of back pressure. Figure 22 displays the values of hydraulic conductivity predicted by the response surface regression for the 9% matrix. Maximum hydraulic conductivity is predicted to be at the highest levels of gradient and back pressure which is different from that observed with the 8% matrix.

Figure 23 is the 2 dimensional contour plot of the response surface regression for the 9% matrix. The K intervals suggest that K is least sensitive to gradient at high levels. This observation must be with reservation, because although the quadratic term of gradient appears as large as the effect of back pressure, it is statistically less significant.

Table 10. Response Surface Regression Analyses

Matrix (wt%)	b_0	b_1	b_2	b_{11}	b_{22}	b_{12}	n	r^2[†]	LOF[§]	p[*]
8	13.01^{**}	2.33^{**}	0.18	-4.30^{**}	-1.21	-0.32	22	0.68	n.s.[#]	0.001
(s.e.)	(0.826)	(0.691)	(0.728)	(1.106)	(1.101)	(0.846)				
9	0.06^{**}	0.023^{**}	0.015^{**}	-0.013	0.003	-0.001	26	0.58	n.s.	0.002
(s.e.)	(0.005)	(0.005)	(0.005)	(0.008)	(0.0077)	(0.0063)				

[†]r^2 = coefficient of determination (variance described by the model)

[§]LOF = Lack of Fit Test

[*]p = probability of a Type I error

** = Significant Effect ($p \leq 0.01$)

[#]n.s. = not significant at $p \leq .05$

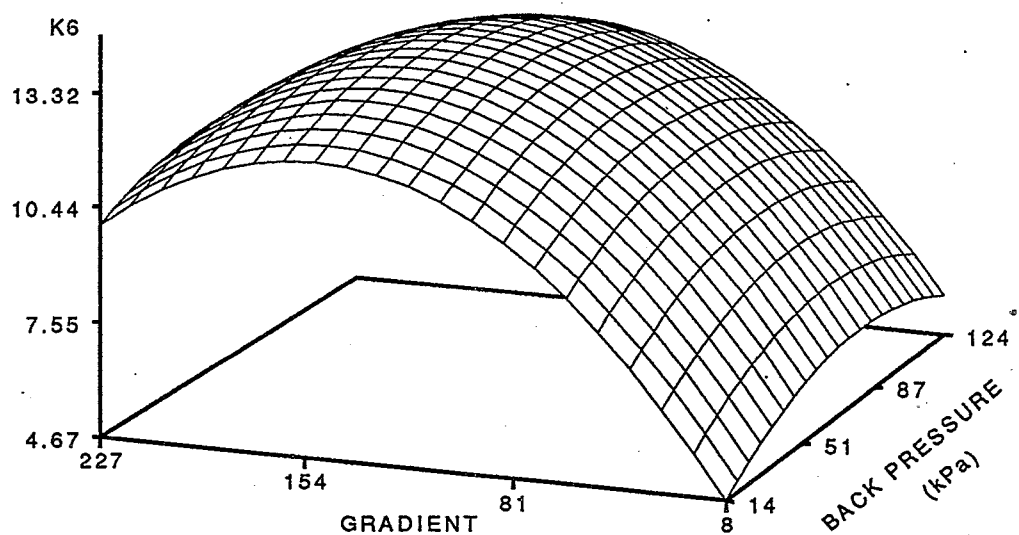FIGURE 20. Response Surface Plot for the 8% Matrix Showing the Predicted Maxima
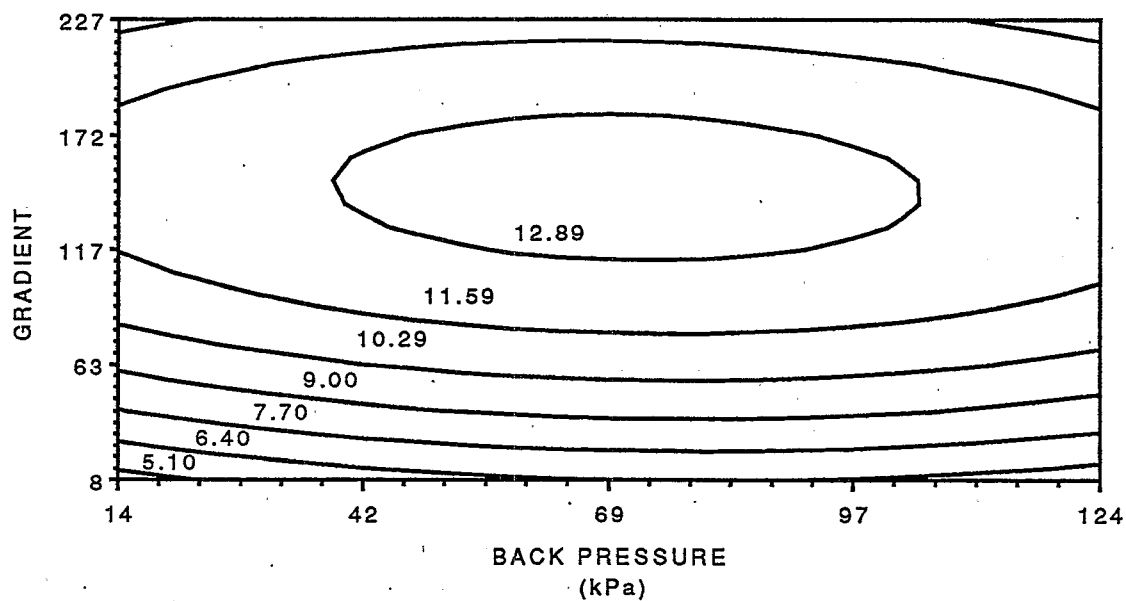

FIGURE 21. Contour Plot of Predicted Values for the 8% Matrix Showing
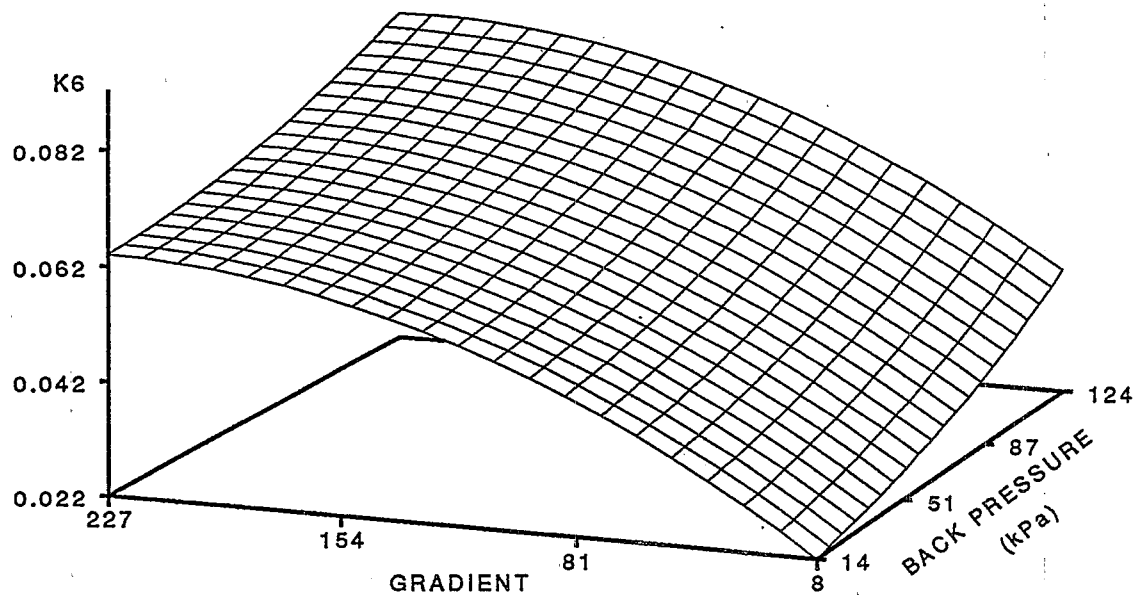Hydraulic Conductivity is Maximized at Median Levels of i and P

FIGURE 22. Response Surface Plot of Predicted Values for the 9% Matrix Showing the Linear Relationship of Gradient and Back Pressure
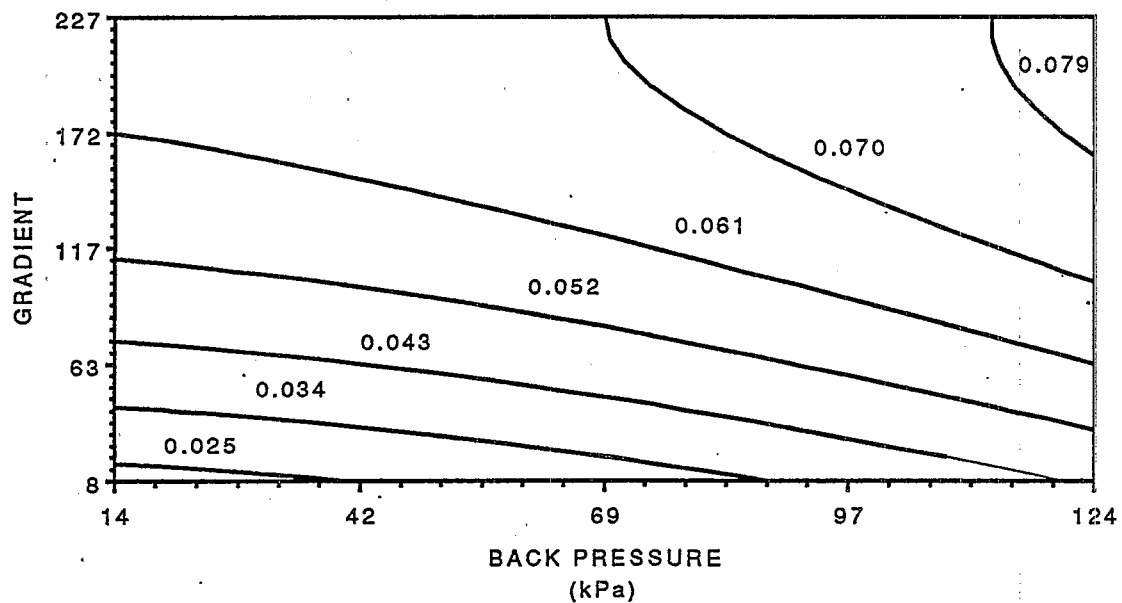

FIGURE 23. Contour Plot of Predicted Values for the 8% Matrix

The variation in hydraulic conductivity was less than four-fold for the 9% matrix and less than three-fold for the 8% matrix as a result of increasing gradient and back pressure from low-levels close to field conditions to the high levels used in accelerated testing. Therefore laboratory measurements conducted to accelerate testing are a reasonable approximation of field conditions. The gradient was varied by a factor of twenty-five while the back pressure was varied by a factor of eight. This relative insensitivity to pressure terms suggests that the samples are highly liquid saturated.

Hydraulic conductivity measurement appears to be most sensitive to gradient at low levels. This has implications for falling-head permeameters which measure hydraulic conductivity at very low gradients where hydraulic conductivity is most sensitive. Regulatory tests could minimize variance by specifying relatively high levels of gradient ($i = 150$, 220 kPa across a 15 cm sample).

The models developed for hydraulic conductivity based on the parameters of gradient and back pressure describe 58% - 68% of the variance in experimental results. A portion of the variance not explained is likely due to the temporal effects noted previously. Linear regression was used to identify equilibrium, when temporal changes in hydraulic conductivity at constant gradient and back pressure (median levels) were not different than zero.

Equilibria were reached by 59, 34 and 27 days for 8, 9 and 10 percent matrices respectively; the null hypothesis, that the estimated slope equalled zero, could not be rejected for any of the three matrices with a probability of Type I error less than 0.13.

This suggests that considering only Type I error may be inappropriate for determining termination criteria for hydraulic conductivity tests. Type II error should be considered in determining hydraulic conductivity equilibria by considering the power of the test. Proper sample size must be determined for an experiment to have sufficient power to detect a given effect size from the null condition with a fixed Type I error rate.

Sample porosities and the equilibrium value of K (mean of trial 5 data after attaining "equilibrium") are shown in Table 11.

Table 11. Sample Porosity

Matrix	Porosity[+]	Pore Volume (cm^3)	Hydraulic Conductivity ($cm.sec^{-1}$)
8%	0.321	236	$(1.36 \pm 0.14) \times 10^{-5}$
9%	0.301	223	$(6.62 \pm 1.44) \times 10^{-8}$
10%	0.272	201	$(3.95 \pm 0.48) \times 10^{-9}$

[+] determined after hydraulic conductivity testing

The samples tested demonstrate a negative correlation between matrix and porosity. Higher cement content is associated with lower sample porosity. Lower sample porosity is also associated with lower hydraulic conductivity.

The relationship of porosity (E) and hydraulic conductivity from Table C.1 (all trial 5 data after attaining "equilibrium" rather than the means) may be modelled according to:

$$K = c \ 10^{bE}$$

where c is a constant and b is the slope of the regression. The coefficients are $c = 2.834 \times 10^{-29}$, and $b = 72.495$ ($r^2 = 0.891$) ($p \leq 0.0001$).

Porosity appears to have some merit as a predictor of hydraulic conductivity. However, bulk porosity does not define pore parameters such as hydraulic radii or whether pores are discrete or capillary.

Cement researchers have studied the relationship of porosity to hydraulic conductivity. Nyame and Illston (16) showed a relationship between hydraulic conductivity and pore structure in cement pastes using hydraulic radius theory. Hydraulic conductivity is related to: $r_h^2 f(E)$ where r_h is the hydraulic radius. This relationship suggests that porosity is not a unique function of hydraulic conductivity. Hughes (17) developed the Poiseuille formula which shows the importance of pore size distribution rather than total porosity. The flow rate across a unit cross section is given by:

$$F = \frac{r^2 \, \Delta \rho \, E}{32 \, N^2 \, \mu \, h}$$

where F is the flow rate ($m^3.sec^{-1}$), r is pore radius (m), $\Delta \rho$ is the pressure difference ($N.m^{-2}$), N is the tortuosity factor, μ is the viscosity ($N.sec.m^{-2}$) and h is the specimen thickness (m). This model was successful in predicting hydraulic conductivity within half an order of magnitude when simplifying assumptions on pore connectivity were made. The dependence of flow on r^2 shows that large pores account for a disproportionate amount of flow. Hydration reactions serve to connect particles as shown above and as suggested by Nyame and Illston (16) subdivide the interstitial space resulting in smaller flow channels. This reduction in flow channel radii may not result in a detectable change in bulk porosity.

In conclusion, porosity has some value as a predictor of hydraulic conductivity within a specific waste/treatment as shown in Table 11. Within a waste/treatment type sample preparation such as additives, compaction and water content etc. may be controlled and the hydraulic conductivity/porosity relationship defined. For between treatment comparisons, independent pore parameters would be required to predict hydraulic conductivity.

SATURATION CONSIDERATIONS

Sample saturation was determined by the ratio of pore water (or free water) to pore volume. Free water was determined as the sample weight loss at 60°C.

Moisture content is a destructive test and thus could only be conducted on test samples after hydraulic conductivity testing. Companion samples prepared under standard conditions were tested to estimate the degree of saturation before subjecting the test samples to standard vacuum saturation. Results from these companion samples and test samples after hydraulic conductivity testing are shown in Table 12.

Table 12. Sample Saturation

Matrix	H_2O (%)	H_2O (cm³)	Pore Volume (cm³)	Saturation (%)
8[+]	4.92	79.5	227.3	35.0
9[+]	5.66	94.2	223.3	42.2
10[+]	6.14	105.4	204.4	51.6
8[*]	12.94	226.5	235.5	96.2
9[*]	11.71	206.4	222.6	92.7
10[*]	10.55	189.6	201.4	94.1

[+] Companion samples after curing

[*] Samples after hydraulic conductivity testing

Results show that samples are highly liquid saturated, which may explain the relative insensitivity of hydraulic conductivity to the instrument pressure parameters discussed previously.

In the field, solidified stabilized wastes will be in the unsaturated state. Flow in solidified/stabilized wastes in the unsaturated state will be different from that measured for saturated wastes in the laboratory. The nature of this unsaturated flow was beyond the scope of this study and should be considered as an area for further research.

Results of the regression analysis showed that the hydraulic conductivity of the solidified/stabilized waste studied responded in a positive linear fashion for both 8% and 9% matrices. A negative quadratic term was significant for the 8% matrix.

Clay and soil-liner researchers suggested that high gradients could lead to sample consolidation and thus lower measured hydraulic conductivity. Bryant and Bodocsi (11) noted that the experimental results of various researchers displayed a negative relationship between hydraulic conductivity and gradient.

The applied gradients for clay and soil liners reported were as high as 300. This would correspond to approximately a 450 kPa pressure drop across a 15 cm sample. A compacted wet clay which had an unconfined compressive strength of 100 kPa would thus be subjected to pressures which would tend to consolidate these samples.

This was not the case with the solidified/stabilized waste studied. The samples studied were molded as monolithic solids with dimensions of 7.62 cm diameter and 15.2 cm height. Companion samples were sacrificed in unconfined compressive strength tests after curing a minimum of forty-one days. Results are summarized in Table 13.

Table 13. Unconfined Compressive Strength Tests (kPA)

| Trial | Matrix | | |
	8 %	9 %	10 %
1	3380	3900	5320
2	3080	3000	6340
3	3830	-	6460
Mean	3430	3450	6040
Standard Deviation	380	640	630

The sample matrices studied displayed an unconfined compressive strength at least ten times greater than the highest pressure drop tested (340 kPa). This may explain the different behaviour noted for solidified/stabilized wastes. The positive correlation of hydraulic conductivity with gradient for solidified/stabilized wastes may represent a response in liquid parameters rather than a response to pore parameters, as is likely the case for clay and soil liners.

REFERENCES

1. Ather, G., Evans, J.C., Fang, H.-Y., and Witmer, K. Influence of Inorganic Permeants upon the Permeability of Bentonite. In: Hydraulic Barriers in Soil and Rock. ASTM STP 874. American Society for Testing and Materials, Philadelphia, 1985. pp 64-73

2. Acar, Y.B., Olivieri, I., and Field, S.D. The Effects of Organic Fluids on Compacted Kaolinite. In: Hydraulic Barriers in Soil and Rock. ASTM STP 874. American Society for Testing and Materials, Philadelphia, 1985. pp 203-212.

3. Fang, H.-Y. and Evans, J.C. Long-Term Permeability Tests Using Leachate on a Compacted Clayey Liner Material. In: Ground-Water Contamination: Field Methods, ASTM STP963. American Society for Testing and Materials, Philadelphia, 1988. pp 397-404.

4. Elzeftawy, A. and Cartwright, K. Evaluating the Saturated and Unsaturated Hydraulic Conductivity of Soils. In: Permeability and Groundwater Contaminant Transport. ASTM STP 746. American Society for Testing and Materials, 1981. pp 168-181.

5. Parker, D.G., Thornton, S.I., and Cheng, C.W. Permeability of Fly-Ash Stabilized Soils. Paper presented at 1977 Specialty Conference of the Geotechnical Engineering Division. American Society of Civil Engineers. Ann Arbour, Michigan. June 13-15, 1977.

6. Carpenter, G.W. and Stephenson, R.W. Permeability Testing in the Triaxial Cell. Geotechnical Testing Journal. 9:1, March 1986. pp 3-9

7.   Edil, T.B. and Erickson, A.E.   Procedure and Equipment Factors Affecting Permeability Testing of a Bentonite-Sand Liner Material. In: Hydraulic Barriers in Soil and Rock.   ASTM STP 874.   American Society for Testing and Materials, Philadelphia, 1985. pp 155-170.

8.   Lentz, R.W., Horst, W.D., and Uppot, J.O. The Permeability of Clay to Acidic and Caustic Permeants. In: Hydraulic Barriers in Soil and Rock. ASTM STP 874. American Society for Testing and Materials, Philadelphia, 1985. pp 127-139.

9.   Bowders, J.J. Termination Criteria for Clay Permeability Testing Discussion. Journal of Geotechnical Engineering. 114:8, 1988. pp 947-950.

10.   Pierce, J.J. and Witter, K.A. Termination Criteria for Clay Permeability Testing. Journal of Geotechnical Engineering. 112:1, 1986. pp 841-854.

11.   Bryant, J. and Bodocsi, A. Precision and Reliability of Laboratory Permeability Measurements. EPA Contract No. 68-03-3210-03 U.S. Environmental Protection Agency, Cincinnati Ohio, 1985. 177 pp.

12.   Pierce, J.J., Salfors, G. and Peterson, E.   Parameter Sensitivity of Hydraulic Conductivity Testing Procedure. Geotechnical Testing Journal. 10:4, December 1987. pp 223-228.

13.   Powers, T.C., Copeland, L.E., Hayes, J.C. and Mann, H.M. Permeability of Portland Cement Paste. Journal of the American Concrete Institute. 26:3, November 1954. pp 285-298.

14.   Powers, T.C., Copeland, L.E. and Mann, H.M. Capillary Continuity or Discontinuity in Cement Pastes. Journal of the Portland Cement Association Research and Development Laboratories. 1:2, May, 1959. pp 38-48.

15. Patel, R.G., Killoh, D.C., Parrott, L.J. and Gutteridge, W.A. Influence of Curing and Different Relative Humidities upon Compound Reactions and Porosity in Portland Cement Paste. Materials and Structures. 21:123, 1988. pp 192-197.

16. Nyame, B.K. and Illston, J.M. Relationships Between Permeability and Pore Structure of Hardened Cement Paste. Magazine of Concrete Research. 33:116, 1981. pp 139-146.

17. Hughes, D.C. Pore Structure and Permeability of Hardened Cement Paste. Magazine of Concrete Research. 37:133, 1985. pp 227-233.

18. Stegemann, J.A. and Cote, P.L. Summary of an Investigation of Test Methods for Solidified Waste Evaluation. Waste Management, 10:1990. pp 41-52.

19. ASTM D-558-82. Standard Test Methods for Moisture-Density Relations of Soil Cement Mixtures. American Society for Testing and Materials. Philadelphia, 1988. V 04.08, pp 108-111.

20. ASTM D2216-80. Standard Test Method for Laboratory Determination of Water Content of Soil, Rock and Soil Aggregate Mixtures American Society for Testing and Materials. Philadelphia, 1988. V 04.08. pp 262-264.

21. ASTM C604-86. Standard Test Method for True Specific Gravity of Refractory Materials by Gas Comparison Pycnometer. American Society for Testing and Materials. Philadelphia, 1988. V 15.01. pp 159-161.

22. ASTM D1633-84. Standard Test Method for Compressive Strength of Molded Soil-Cement Cylinders. American Society for Testing and Materials. Philadelphia, 1988. V 04.08. pp 229-231.

23.   AWWA #209A. Total Residue Dried at 103 - 105°C In: Standard Methods for the Examination of Water and Wastewater. 15th Ed. American Water Works Association. Washington D.C., 1981. pp 93-94.

24.   SAS Institute Inc. SAS/STAT User's Guide. Release 6.03 Edition. Cary, NC:SAS Institute Inc., 1988. 1028 pp.

25.   Garcia-Bengochea, I. and Lovel, C.W. Correlative Measurements of Pore Site Distribution and Permeability in Soils. In: Permeability and Ground Water Transport. ASTM STP 746. American Society for Testing and Materials. Philadelphia, 1981. pp 137-150.

26.   Dalgleish, B.J. and Pratt, P.L. Fractographic Studies of Microstructural Development in Hydrated Portland Cement. Journal of Materials Science. 17:8, 1982. pp 2199-2207.

APPENDIX A

CALIBRATION OF GEOTEST PERMEAMETER INTERFACES

Calibration of the Geotest interface was conducted by measuring the mass of water expelled from the interface as a function of interface piston displacement. Linear regression was used to determine the linear displacement/mass response of the interface, used in subsequent hydraulic conductivity determinations.

Equipment required included a: Geotest Interface (Model S5425), Mitutoyo Digimatic Indicator (Type ID-130ME), Mitutoyo miniprocessor (DP2-DX), Mettler analytical balance (HK 160) with RS232 Adapter (Mettler CL249) and computer (Fujikama Model #fk286MT). The equipment layout is shown in Figure A.1.

Open containers of water with paper towel wicks were placed in the balance weighing chamber twenty minutes before commencing the calibration to saturate the local environment and minimize evaporation loss. Twenty data points were collected at each of 6, 12, 18 and 24 mm interface piston displacements. Eighty data points were generated by discharging ~ 0.012 g of water into a 50 ml volumetric flask with a corresponding piston displacement of ~ 0.006 mm.

Data collected were merged into a single file by matching time readings from the Data Logger and Balance files. Data in an ASCII format was imported into SAS (1988 Release 6.03) for statistical analysis. A least squares estimate for a linear model of interface piston displacement versus mass of water was produced.

Calibrations were performed three times over a fifteen month period; an initial calibration, prior to, and at the end of hydraulic conductivity experiments. The results of the three calibrations for the six interfaces are shown in Table A.1.
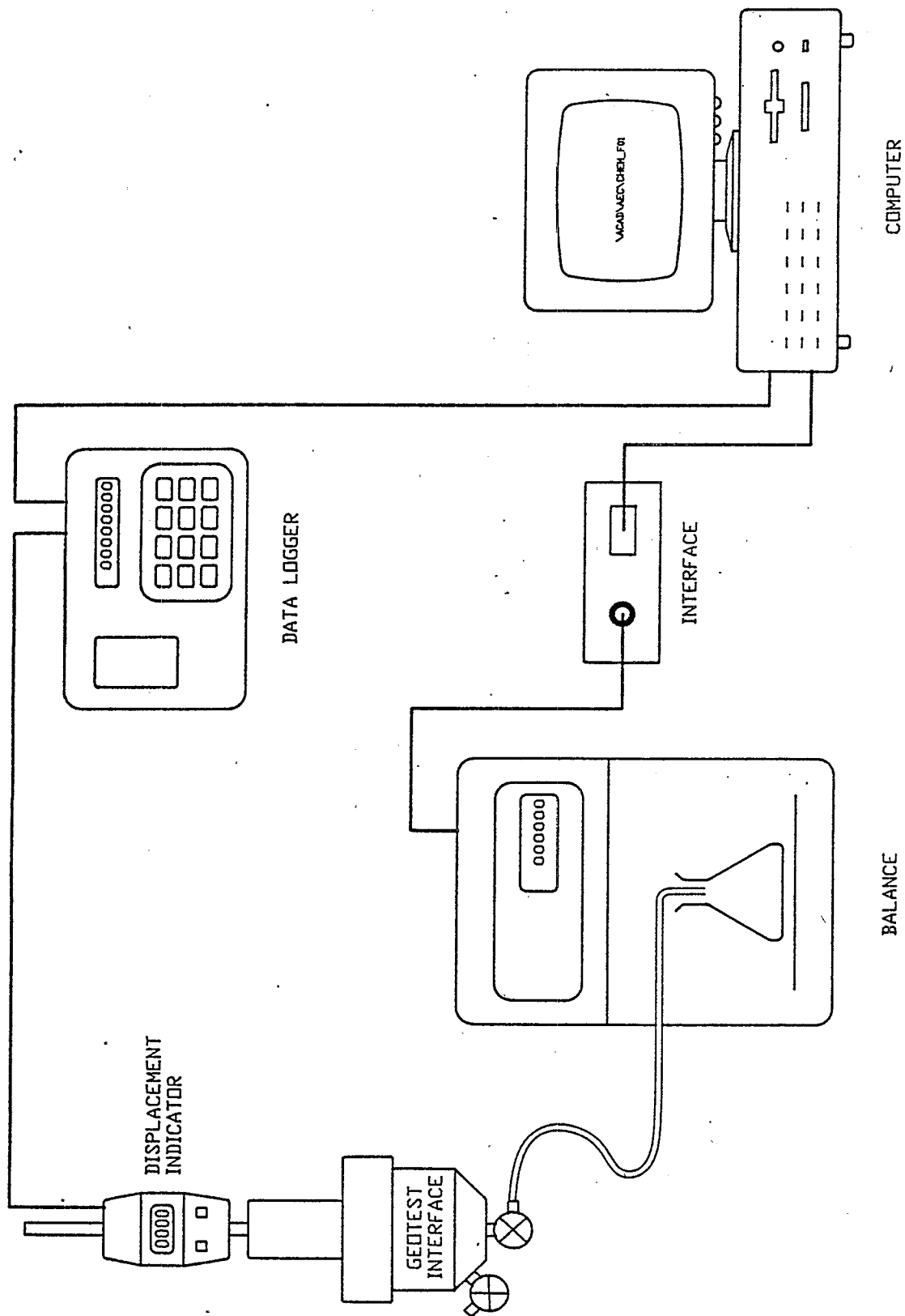
FIGURE A.1 Apparatus for Calibration of Geotest Permeameter Interfaces

The points fit the linear model sufficiently well to generate a coefficient of determination of 1.0000. The standard error in the slope was less than 0.011% in all cases. The deviation from the linear model was determined for each interface calibration. The maximum residual deviation was +0.0079 mm and -0.0077 mm. The predicted residual from the sum of squares was a maximum of 0.0033 mm, which represents the machine error.

Table A.1. Interface Calibrations

Interface #		Slope # (mm.g^{-1})	Std. Error of Slope
761	1	0.500373	0.000032
	2	0.500949	0.000015
	3	0.502044	0.000026
925	1	0.502238	0.000017
	2	0.502361	0.000055
	3	0.501614	0.000029
926	1	0.499960	0.000051
	2	0.500320	0.000034
	3	0.501395	0.000011
928	1	0.501553	0.000008
	2	0.502538	0.000027
	3	0.503015	0.000014
929	1	0.501781	0.000022
	2	0.501484	0.000020
	3	0.501940	0.000020
930	1	0.502952	0.000032
	2	0.504165	0.000013
	3	0.502900	0.000035

IN-HOUSE COMPUTER PROGRAM

The computer program accepted data from the Miniprocessor and stored it in a file on the hard drive. The program included several options for calibration, hydraulic conductivity calculation and file management. The file name was coded to the Geotest interface serial # and the date of data acquisition. An example is shown below:

761_1D90.019

This file indicates the: Mitutoyo Indicator serial number, file status (original or edited), file number of day, file type (balance file, data file, merged balance and data calibration file, or hydraulic conductivity calibration file), year and Julian day.

A header on the data file recorded the experimental conditions (trial #, gradient, back pressure and matrix) and the sample/test series numbers.

A test pressure file was coded with the sample/test series number and contains the test values for the head, back and cell pressures.

The sample file was coded to the sample number and contained the sample dimensions, weight, moisture content and sample preparation compositions.

The hydraulic conductivity calculation incorporated data from the sample, pressure and data files. The hydraulic conductivity could be calculated for the entire data file or at a specified time interval between any two data points. The hydraulic conductivity calculation is shown below:

$$K = \frac{(D_2 - D_1) \cdot L \cdot 4}{S \cdot \rho \, (HP - BP) \cdot PH \cdot \pi \, (OD \cdot 2.54)^2 \, (t_2 - t_1)}$$

D = Interface displacement (mm)

S = Slope of calibration curve from regression analysis (mm/g)

ρ = Water density at 24°C (0.9973 g/cm^3)

L = Mean sample length (cm)

HP = Head pressure (psi)

BP = Back pressure (psi)

PH = Pressure to head conversion (70.47 cm water/psi)

OD = Mean outside diameter (in.)

t = Time of displacement reading (sec.)

EXPERIMENTAL DATA

Table C.1. Hydraulic Conductivity Results

JULIAN DAY	TEST DAY	LOG TEST DAY	MATRIX	TRIAL	i	P	K	LOG K	VOLUME	Σ VOLUME	TDS⁺	VWTDS*	Σ VWTDS
163	0		8	5	0	0	8.02E-05	-4.09583	37.3	37.3	66.00	2.462	2.46
169	6	0.78	8	5	0	0	4.45E-05	-4.35164	40.8	78.1	58.00	2.366	4.83
176	13	1.11	8	5	0	0	3.53E-05	-4.45223	33.7	111.8	62.30	2.100	6.93
184	21	1.32	8	5	0	0	2.09E-05	-4.67985	29.9	141.7	57.70	1.725	8.65
190	27	1.43	8	5	0	0	1.95E-05	-4.70997	32.3	174	50.50	1.631	10.28
197	34	1.53	8	5	0	0	1.41E-05	-4.85078	32.0	206	43.30	1.386	11.67
204	41	1.61	8	5	0	0	9.45E-06	-5.02457	30.2	236.2	37.90	1.145	12.81
208	45	1.65	8	3	1	-1	9.93E-06	-5.00305	32.1	268.3	32.70	1.050	13.87
211	48	1.68	8	4	0	1	9.18E-06	-5.03716	31.3	299.6	25.60	0.801	14.67
222	59	1.77	8	5	0	0	1.41E-05	-4.85078	53.8	353.4	20.80	1.119	15.79
225	62	1.79	8	1	1	1	1.26E-05	-4.89963	26.3	379.7	18.20	0.479	16.26
227	64	1.81	8	8	-1	0	2.54E-06	-5.59517	19.5	399.2	16.70	0.326	16.59
228	65	1.81	8	2	1	0	1.28E-05	-4.89279	46.5	445.7	13.00	0.605	17.20
229	66	1.82	8	9	-1	-1	1.67E-06	-5.77728		452.8			
233	70	1.85	8	5	0	0	1.54E-05	-4.81248	35.8	481.5	11.00	0.394	17.59
234	71	1.85	8	5	0	0	1.46E-05	-4.83565	35.7	517.2	9.60	0.343	17.93
235	72	1.86	8	5	0	0	1.43E-05	-4.84466	68.4	585.6	6.50	0.445	18.38
239	76	1.88	8	5	0	0	1.32E-05	-4.87943	34.1	619.7	6.40	0.218	18.59
241	77	1.89	8	5	0	0	1.28E-05	-4.89279	34.1	653.8	6.30	0.215	18.81
244	81	1.91	8	7	-1	1	8.07E-06	-5.09313	33.8	687.6	5.90	0.199	19.01
253	90	1.95	8	3	1	-1	9.84E-06	-5.007	64.3	751.9	5.60	0.360	19.37
254	91	1.96	8	4	0	1	1.07E-05	-4.97062	34.1	786	5.20	0.177	19.55
255	92	1.96	8	6	0	-1	1.09E-05	-4.96257	34.2	820.2	3.90	0.133	19.68
256	93	1.97	8	5	0	0	1.15E-05	-4.9393	62.0	882.2	3.80	0.236	19.91
257	94	1.97	8	7	-1	1	5.86E-06	-5.2321	30.5	912.7	3.60	0.110	20.02
261	98	1.99	8	8	-1	0	6.75E-06	-5.1707	76.1	988.8	3.80	0.289	20.31
264	101	2.00	8	9	-1	-1	8.61E-06	-5.065	27.5	1016.3	3.50	0.096	20.41
270	107	2.03	8	2	1	0	7.98E-06	-5.098	33.3	1049.6	3.50	0.117	20.53
271	108	2.03	8	1	1	1	8.28E-06	-5.08197	17.1	1066.7	3.10	0.053	20.58
163	0		9	5	0	0	1.56E-06	-5.80688	36.5	36.5	97.00	3.541	3.54
169	6	0.78	9	5	0	0	4.85E-07	-6.31426	41.5	78.	91.00	3.776	7.32
176	13	1.11	9	5	0	0	2.07E-07	-6.68403	29.6	107.6	91.30	2.702	10.02
184	21	1.32	9	5	0	0	1.17E-07	-6.93181	14.3	121.9	87.30	1.248	11.27
190	27	1.43	9	5	0	0	8.00E-08	-7.09691		132.7			
197	34	1.53	9	5	0	0	6.20E-08	-7.20761	18.9	140.8	85.70	1.620	12.89
204	41	1.61	9	5	0	0	5.10E-08	-7.29243	7.1	147.9	66.00	0.469	13.36
208	45	1.65	9	3	1	-1	7.27E-08	-7.13847		152.8			

(TABLE C.1 continued)

JULIAN DAY	TEST DAY	LOG TEST DAY	MATRIX	TRIAL	i	P	K	LOG K	VOLUME	Σ VOLUME	TDS+	VWTDS*	Σ VWTDS
211	48	1.68	9	4	0	1	5.66E-08	-7.24718	12.9	160.8	63.80	0.823	14.18
213	50	1.70	9	6	0	-1	3.62E-08	-7.44129	12.0	172.8	57.20	0.686	14.87
222	59	1.77	9	5	0	0	1.02E-07	-6.9914	27.1	199.9	42.30	1.146	16.01
225	62	1.79	9	1	1	1	1.14E-07	-6.9431		214.5			
228	65	1.81	9	2	1	0	8.60E-08	-7.0655	41.8	241.7	36.00	1.505	17.52
232	69	1.84	9	9	-1	-1	1.78E-08	-7.74958		244			
234	71	1.85	9	5	0	0	6.19E-08	-7.20831	33.3	275	31.70	1.056	18.57
235	72	1.86	9	5	0	0	5.62E-08	-7.25026	28.0	303	26.90	0.753	19.32
236	73	1.86	9	5	0	0	5.68E-08	-7.24565	33.4	336.4	20.70	0.691	20.02
240	77	1.89	9	5	0	0	5.96E-08	-7.22475	28.4	364.8	16.20	0.460	20.48
241	78	1.89	9	5	0	0	6.91E-08	-7.16052	33.6	398.4	13.20	0.444	20.92
242	79	1.90	9	5	0	0	6.48E-08	-7.18842	33.0	431.4	11.00	0.363	21.28
246	83	1.92	9	7	0	1	3.53E-08	-7.45223		436.1			
250	87	1.94	9	8	-1	0	1.73E-08	-7.76195		437.8			
253	90	1.95	9	3	-1	-1	6.39E-08	-7.1945	20.5	451.9	9.70	0.199	21.48
254	91	1.96	9	4	0	1	8.43E-08	-7.07417	11.3	463.2			
255	92	1.96	9	6	0	-1	4.57E-08	-7.34008	6.9	470.1	9.70	0.067	21.55
256	93	1.97	9	5	0	0	7.48E-08	-7.1261	11.0	481.1			
260	97	1.99	9	7	-1	1	5.95E-08	-7.22548	7.9	489	9.10	0.072	21.62
264	101	2.00	9	8	1	0	2.55E-08	-7.59346		521.4			
270	107	2.03	9	2	1	0	7.21E-08	-7.14206		535.1			
271	108	2.03	9	1	1	1	7.81E-08	-7.10735		550.7			
274	111	2.05	9	9	-1	-1	1.30E-08	-7.88606	61.8	550.8	7.00	0.433	22.05
166	3	0.48	10	5	0	0	1.73E-07	-6.76195		41.3			
169	6	0.78	10	5	0	0	8.39E-08	-7.07624		51.6			
176	13	1.11	10	5	0	0	2.73E-08	-7.56384		55.4			
184	21	1.32	10	5	0	0	9.74E-09	-8.01144		56.7			
190	27	1.43	10	5	0	0	5.49E-09	-8.26043		57.6			
197	34	1.53	10	5	0	0	3.53E-09	-8.45223	57.7	57.7	128.00	7.386	7.39
198	35	1.54	10	5	0	0	3.61E-09	-8.44249		77.9			
204	41	1.61	10	5	0	0	4.09E-09	-8.38828		78.8			
208	45	1.65	10	3	-1	-1	3.18E-09	-8.49757		82.1			
212	49	1.69	10	4	0	1	2.98E-09	-8.52578		84.2			
214	51	1.71	10	6	0	-1	1.20E-09	-8.92082		86.5			
220	57	1.76	10	7	-1	1	1.65E-08	-7.78252		90.2			
225	62	1.79	10	5	0	1	4.58E-09	-8.33913		108.6			
226	63	1.80	10	1	1	1	4.58E-09	-8.33913		113.5			
229	66	1.82	10	2	1	0	4.55E-09	-8.34199	59.0	116.7	144.00	8.496	15.88
241	78	1.89	10	2	1	0	2.09E-09	-8.67985	34.0	150.7	123.00	4.182	20.06

+ Total Dissolved Solids (g/L)
* Volume Weighted Total Dissolved Solids (g)

Table C.2. 8% Matrix Replicate Data

Test Day	K930 (cm.sec^{-1})	K928 (cm.sec^{-1})	K925 (cm.sec^{-1})	LOG K930	LOG K928	LOG K925
1	1.37E-04	1.67E-04	7.40E-05	-3.863	-3.777	-4.131
5	1.02E-04	8.20E-05	3.20E-05	-3.991	-4.086	-4.495
8	8.22E-05	5.46E-05	2.66E-05	-4.085	-4.263	-4.575
12	6.63E-05	4.19E-05	2.29E-05	-4.178	-4.378	-4.640
15	5.64E-05	3.45E-05	1.93E-05	-4.249	-4.462	-4.714
19	4.75E-05	2.78E-05	1.67E-05	-4.323	-4.556	-4.777
22	4.15E-05	2.38E-05	1.47E-05	-4.382	-4.623	-4.833
25	3.68E-05	2.02E-05	1.28E-05	-4.434	-4.695	-4.893
26	3.49E-05	1.92E-05	1.19E-05	-4.457	-4.717	-4.924
27	3.24E-05	1.74E-05	1.07E-05	-4.489	-4.759	-4.971
28	3.08E-05	1.66E-05	9.96E-06	-4.511	-4.780	-5.002
29	2.96E-05	1.59E-05	9.61E-06	-4.529	-4.799	-5.017
Mean	5.81 x 10^{-5}	4.34 x 10^{-5}	2.18 x 10^{-5}	-4.29	-4.49	-4.75
Std. Deviation	3.36 x 10^{-5}	4.36 x 10^{-5}	1.79 x 10^{-5}	0.22	0.32	0.26
Normality Test Value[*]	2.03	9.02	6.40	1.08	1.30	1.28

[*] Critical Values 1.36 (α = 0.10), 1.72 (α = 0.05)

DC/ps

ET-CW

2440-CW

91.06.21